17-AAG functions with preserved UPS function

As we demonstrated in an in vitro study, 17-AAG-induced degradation requires a well-preserved proteasome function [15]. However, a question concerning the usefulness of this pharmacological approach to facilitate a self-clearing system has been raised [62]. It is generally accepted that the ubiquitin–proteasome system (UPS) is strongly involved in the pathology of polyQ diseases, as many components of the ubiquitin–proteasome and molecular chaperones are known to co-localize with polyQ-containing NIs [63, 64]. Previous reports of studies performed in cultured cell models suggested that an impairment of the UPS is probably a common pathology in polyQ diseases [65–67]. If this hypothesis were true, 17-AAG could not exert its pharmacological effect on polyQ diseases; its therapeutic effects are dependent on a preserved proteasome function [15, 47, 48, 62].

In this regard, recent studies using in vivo proteasome assays have raised serious questions concerning the impaired UPS hypothesis of polyQ diseases [68–70]. It has been reported that neuronal dysfunction developed without significant impairment of the UPS in a mouse model of SCA7 [69]. Consistent with this, it was also demonstrated that proteasome impairment did not contribute to pathogenesis in a mouse model of Huntington's disease (HD) [70]. Furthermore, in conditional mouse models of polyQ disease, genetic loss of the abnormal gene product led to a rapid clearance of pre-existing polyQ-mediated NIs and reversible improvement of the abnormal phenotypes [71, 72]. If the UPS were irreversibly damaged in polyQ diseases, then pre-existing NIs could not be diminished.

While it remains unclear what the difference is in proteasome function in in vitro and in vivo models, our research in a mouse model of SBMA indicates that impairment of the UPS is not a major etiology, at least in in vivo models of polyQ diseases. We therefore consider that treatment with 17-AAG, which takes advantage of a self-clearing system to target disease-causing proteins, is a reasonable therapeutic strategy against polyQ-related and other neurodegenerative diseases.

The expected beneficial effects of 17-AAG against other neurodegenerative diseases

Among neurodegenerative-disease-causing proteins, only AR in SBMA is established as an Hsp90 client protein at this time. It will be interesting to assess whether other neurodegenerative-disease-causing proteins also belong to the family of Hsp90 client proteins. Recent studies have already revealed that some Hsp90 client proteins exerted adverse influences on several neurological disorders [73–75], indicating that the clinical application of Hsp90 inhibitors could expand beyond the treatment of oncological diseases. With reference to previous reports, we now discuss the possibility that 17-AAG could be applicable to neurodegeneration other than SBMA (Fig. 4).

Using 17-AAG as an inducer of HSPs

Hsp90 inhibitors are known to possess the unique pharmacological effect of inducing a stress response and, in addition to their use as anti-cancer agents, have also been developed as pharmacological HSP inducers [52, 76]. This pharmacological effect has already been confirmed in human clinical trials [22]. Murakami et al. were the first to show that the Hsp90 inhibitor herbimycin had the ability to induce Hsp70 in various cultured cell models [77]. Thereafter, Hsp90 proved to be a repressor of heat transcription factor (HSF-1) [78]. Hsp90 inhibitors cause a disassociation of HSF-1 from the Hsp90 complex and a trimerization of HSF-1, thereby resulting in HSP activation. Based on the ability to induce HSPs, Hsp90 inhibitors have also been applied to non-oncological diseases [52].

A great number of reports revealed that forced overexpression of Hsp70 resulted in acquisition of tolerance against various types of stresses and protection against apoptosis in various disease models [79]. In a wide range of polyQ disease models, both genetic and pharmacological overexpression of HSPs has been shown to suppress aggregate formation and cellular toxicity [63, 80, 81]. There is no doubt that HSP induction is beneficial for various neurodegenerative diseases [54]. We have also demonstrated that both genetic and pharmacological overexpression of Hsp70 significantly ameliorated expression of the abnormal phenotype in a transgenic mouse model of SBMA [40, 82].

Taking advantage of HSP induction, many studies have already showed that Hsp90 inhibitors exerted potential neuroprotective effects in: a model of HD [57, 83, 84], tauopathies [28, 85–87], Parkinson's disease [88–90], stroke [91, 92], and autoimmune encephalomyelitis [93]. In addition, Hsp90 inhibitors themselves have been shown to have some neuroprotective effects against various stresses, such as drug-induced toxicity, oxidative stress, and oxygen-glucose deprivation [94–97]. As for polyQ diseases, Sittler et al. [57] first showed that GA significantly suppressed aggregation of mutant huntingtin in a cultured cell model of HD via induction of the Hsp70 and Hsp40 heat shock response. Thus, the enhancement of cellular defenses using Hsp90 inhibitors is a very reasonable clinical application for neurodegenerative diseases.

In polyQ diseases, Bates and his colleagues [83] showed a progressive decrease in the expression of Hsp70 and Hsp40 in a mouse model of HD, which was also observed in our SBMA model [82]. The ability of Hsp90 inhibitors to significantly induce HSPs has been demonstrated only in cultured cell models and in the fly model, but not in mammals. Therefore, further investigation should be performed to address how much Hsp90 inhibitors can induce HSPs in mouse models of neurodegenerative disorders other than SBMA. Although it appears to be obvious that it would be advantageous for the treatment of neurodegeneration, in inducing HSPs by Hsp90 inhibitors, in view of our research finding in in vivo models, it would be unadvisable to rely only on the induction of nonspecific HSPs for human clinical trials.

Using 17-AAG as a kinase inhibitor in neurodegeneration

Phosphorylated tau is a representative disease-causing protein associated with tauopathies including fronto-temporal dementia, progressive supranuclear palsy, corticobasal degeneration, and multiple system atrophy. It is interesting to note that phosphorylated tau is a targeted protein of Hsp90 inhibitors [28, 85, 86]. Dou et al. recently showed that GA and 17-AAG indirectly blocked abnormal tau phosphorylation by inhibition of the Raf–MEK–extracellular signal-regulated kinase (ERK) pathway [98], of which upstream kinase Raf is also an Hsp90 client protein [10, 99]. ERK is known to mediate the activation and stabilization of phosphorylated tau [100, 101]. Along these same lines, LaFevre-Bernt and Ellerby [102] demonstrated that polyQ-expanded, mutant-AR-mediated neuronal cell death by ERK activation and that selective inhibition of the ERK pathway reduced polyQ-induced cell death. Based on this mechanism of inhibiting ERK activation, 17-AAG might also ameliorate abnormal phenotypic expression in the mouse model of SBMA. Furthermore, in other neurodegenerative disorders, evidence has accumulated suggesting that ERK activation is an important executor of neuronal damage [103–106]. Hsp90 inhibitors are well known to have the ability to inhibit various kinase activity [10]. This pharmacological effect of Hsp90 inhibitors, to reduce abnormal kinase activity, could be applied to neurodegenerative diseases as well as oncological diseases and could have far-reaching influence on the clinical application of Hsp90 inhibitors.

Zoghbi and colleagues demonstrated that Akt/PI3K was essential for stabilization and accumulation of mutant ataxin-1 in the polyQ-associated disease SCA1 [73, 107]. Akt is also an Hsp90 client protein, whose activity is significantly reduced by Hsp90 inhibition [108, 109]. Thus, reduction of Akt kinases activity by Hsp90 inhibition might be a therapeutic approach for SCA1. Although Akt/PI3K is believed to be a major pathway mediating survival signals in neuronal cells [110], their finding raises an issue about this hypothesis.

Hsp90 inhibitors have been found to have some neuroprotective effects such as on axonal regeneration in cultured cell models [94, 111]. Koprivica et al. demonstrated that epidermal growth factor receptor (EGFR) activation mediates inhibition of axon regeneration [74]. That EGFR is also an Hsp90 client protein [112, 113] might help explain how Hsp90 inhibition is related to axonal regeneration. In another example, GA markedly attenuates ischemic brain damage [91, 92] and IκB kinase (IKK), an Hsp90 client protein [114], plays an important role in ischemia-induced neuronal death [75, 115], suggesting that GA may ameliorate ischemia brain damage by reducing IKK activity as well as by inducing HSPs.

There is a caveat to this suggestion, however. If 17-AAG is to be applied clinically to treat neurodegenerative diseases with the expectation of reducing abnormal kinase activity, we should also keep in mind the possibility that 17-AAG might also inhibit some kinase activation that exerts cytoprotective effects against neuron degeneration. Taking HD as an example, the efficacy of GA has already been shown based on its ability to induce HSPs [57, 83]. However, a report recently released by Apostol et al. showed that ERK1/2 activation protects against mutant huntingtin-induced toxicity [116]. Furthermore, in a cultured cell model of HD carrying full-length huntingtin, various kinase activities were inhibited by mutant polyQ-expanded huntingtin, but not by normal huntingtin [117, 118]. If ERK activation plays a major role in protecting against HD phenotype expression, there is concern that 17-AAG might exert an adverse affect on HD by inhibiting ERK activation. Before applying 17-AAG to a neurological disorder, we should assess whether the kinase targeted by Hsp90 inhibitor is a true exacerbating factor for the pathology. While there may be some debate over whether 17-AAG should be used as a kinase inhibitor in neurodegeneration, if the application of 17-AAG is suitably performed, this agent would be expected to effectively inhibit abnormal kinase activity in several neurological disorders, possibly leading to cures for these diseases. Hence, this strategy is also of value to extend the versatility of Hsp90 inhibitors as therapeutic agents for neurological disorders.

Conclusion

When considering a role for molecular chaperones in neurological disorders, it should be said that Hsp70 and Hsp40 have received most of the attention, especially in neurodegenerative diseases, as these chaperones have the desirable ability to refold abnormal proteins or to carry them to degradation as a part of the system of protein quality control [54, 119]. Compared with this, Hsp90 is not known to directly fold non-native proteins but rather to bind to substrate proteins only at a late stage of folding [120]. Considering our research findings and those of the other above-mentioned reports, in addition to its role in malignancies, Hsp90 exerts an adverse influence on the nervous system in some situations. In this case, it is reasonable to consider modulating Hsp90 function appropriately.

The ability of 17-AAG to facilitate the degradation of abnormal toxic protein through the modulation of Hsp90 function would be directly applicable to SBMA and probably other neurodegenerative disorders as well. But we should keep in mind that 17-AAG is not a panacea for neurological disorders because it has only limited ability to induce Hsp70 and Hsp40 in vivo. 17-AAG is expected to exert the most effective therapeutic potential against diseases in which the main etiological factor is mediated by Hsp90 client proteins, like AR in SBMA. We believe that more research should be invested in examining the effects of Hsp90 inhibitors on neurodegeneration and that suitably modulating Hsp90 function has great potential to become a new molecular-targeted therapy against a wide range of neurodegenerative diseases.

Acknowledgements We thank the National Cancer Institute and Kosan Biosciences for kindly providing 17-AAG. This work was supported by a Center-of-Excellence (COE) grant from the Ministry of Education, Culture, Sports, Science and Technology, Japan, by grants from the Ministry of Health, Labur, and Welfare, Japan, by a grant from the Naito Foundation, and by a grant from the Kanae Foundation.

References

1. Di Prospero NA, Fischbeck KH (2005) Therapeutics development for triplet repeat expansion diseases. Nat Rev Genet 6:756–765
2. La Spada AR, Wilson EM, Lubahn DB, Harding AE, Fischbeck KH (1991) Androgen receptor gene mutations in X-linked spinal and bulbar muscular atrophy. Nature 352:77–79
3. Sobue G, Hashizume Y, Mukai E, Hirayama M, Mitsuma T, Takahashi A (1989) X-linked recessive bulbospinal neuronopathy. A clinicopathological study. Brain 112(Pt 1):209–232
4. Tanaka F, Doyu M, Ito Y, Matsumoto M, Mitsuma T, Abe K, Aoki M, Itoyama Y, Fischbeck KH, Sobue G (1996) Founder effect in spinal and bulbar muscular atrophy (SBMA). Hum Mol Genet 5:1253–1257
5. Doyu M, Sobue G, Mukai E, Kachi T, Yasuda T, Mitsuma T, Takahashi A (1992) Severity of X-linked recessive bulbospinal neuronopathy correlates with size of the tandem CAG repeat in androgen receptor gene. Ann Neurol 32:707–710
6. Adachi H, Katsuno M, Minamiyama M, Waza M, Sang C, Nakagomi Y, Kobayashi Y, Tanaka F, Doyu M, Inukai A, Yoshida M, Hashizume Y, Sobue G (2005) Widespread nuclear and cytoplasmic accumulation of mutant androgen receptor in SBMA patients. Brain 128:659–670
7. Fang Y, Fliss AE, Robins DM, Caplan AJ (1996) Hsp90 regulates androgen receptor hormone binding affinity in vivo. J Biol Chem 271:28697–28702
8. Georget V, Terouanne B, Nicolas JC, Sultan C (2002) Mechanism of antiandrogen action: key role of hsp90 in conformational change and transcriptional activity of the androgen receptor. Biochemistry 41:11824–11831
9. Poletti A (2004) The polyglutamine tract of androgen receptor: from functions to dysfunctions in motor neurons. Front Neuroendocrinol 25:1–26
10. Pratt WB, Toft DO (2003) Regulation of signaling protein function and trafficking by the hsp90/hsp70-based chaperone machinery. Exp Biol Med (Maywood) 228:111–133
11. Neckers L (2002) Hsp90 inhibitors as novel cancer chemotherapeutic agents. Trends Mol Med 8:S55–S61
12. Vanaja DK, Mitchell SH, Toft DO, Young CY (2002) Effect of geldanamycin on androgen receptor function and stability. Cell Stress Chaperones 7:55–64
13. Solit DB, Zheng FF, Drobnjak M, Munster PN, Higgins B, Verbel D, Heller G, Tong W, Cordon-Cardo C, Agus DB, Scher HI, Rosen N (2002) 17-Allylamino-17-demethoxygeldanamycin induces the degradation of androgen receptor and HER-2/neu and inhibits the growth of prostate cancer xenografts. Clin Cancer Res 8:986–993
14. Neckers L (2002) Heat shock protein 90 inhibition by 17-allylamino-17- demethoxygeldanamycin: a novel therapeutic approach for treating hormone-refractory prostate cancer. Clin Cancer Res 8:962–966
15. Waza M, Adachi H, Katsuno M, Minamiyama M, Sang C, Tanaka F, Inukai A, Doyu M, Sobue G (2005) 17-AAG, an Hsp90 inhibitor, ameliorates polyglutamine-mediated motor neuron degeneration. Nat Med 11:1088–1095
16. DeBoer CMP, Wnuk RJ, Peterson DH (1970) Geldanamycin, a new antibiotic. J Antibiot (Tokyo) 23:442–447
17. Whitesell L, Shifrin SD, Schwab G, Neckers LM (1992) Benzoquinonoid ansamycins possess selective tumoricidal activity unrelated to src kinase inhibition. Cancer Res 52: 1721–1728
18. Neckers L, Schulte TW, Mimnaugh E (1999) Geldanamycin as a potential anti-cancer agent: its molecular target and biochemical activity. Invest New Drugs 17:361–373
19. Supko JG, Hickman RL, Grever MR, Malspeis L (1995) Preclinical pharmacologic evaluation of geldanamycin as an antitumor agent. Cancer Chemother Pharmacol 36:305–315
20. Schulte TW, Neckers LM (1998) The benzoquinone ansamycin 17-allylamino-17-demethoxygeldanamycin binds to HSP90 and shares important biologic activities with geldanamycin. Cancer Chemother Pharmacol 42:273–279
21. Page J, Heath J, Fulton R, Yalkowsky E, Tabibi E, Tomaszewski J, Smith A, Rodman L (1997) Comparison of geldanamycin (NSC-122750) and 17-allylaminogeldanamycin (NSC-330507D) toxicity in rats. Proc Am Assoc Cancer Res 38:308
22. Goetz MP, Toft D, Reid J, Ames M, Stensgard B, Safgren S, Adjei AA, Sloan J, Atherton P, Vasile V, Salazaar S, Adjei A, Croghan G, Erlichman C (2005) Phase I trial of 17-allylamino-17-demethoxygeldanamycin in patients with advanced cancer. J Clin Oncol 23:1078–1087
23. Banerji U, O'Donnell A, Scurr M, Pacey S, Stapleton S, Asad Y, Simmons L, Maloney A, Raynaud F, Campbell M, Walton M, Lakhani S, Kaye S, Workman P, Judson I (2005) Phase I pharmacokinetic and pharmacodynamic study of 17-allylamino, 17-demethoxygeldanamycin in patients with advanced malignancies. J Clin Oncol 23:4152—4161
24. Grem JL, Morrison G, Guo XD, Agnew E, Takimoto CH, Thomas R, Szabo E, Grochow L, Grollman F, Hamilton JM, Neckers L, Wilson RH (2005) Phase I and pharmacologic study of 17-(allylamino)-17-demethoxygeldanamycin in adult patients with solid tumors. J Clin Oncol 23:1885–1893
25. Ramanathan RK, Trump DL, Eiseman JL, Belani CP, Agarwala SS, Zuhowski EG, Lan J, Potter DM, Ivy SP, Ramalingam S, Brufsky AM, Wong MK, Tutchko S, Egorin MJ (2005) Phase I pharmacokinetic–pharmacodynamic study of 17-(allylamino)-17-demethoxygeldanamycin (17-AAG, NSC 330507), a novel inhibitor of heat shock protein 90, in patients with refractory advanced cancers. Clin Cancer Res 11:3385–3391
26. Heath EI, Gaskins M, Pitot HC, Pili R, Tan W, Marschke R, Liu G, Hillman D, Sarkar F, Sheng S, Erlichman C, Ivy P (2005) A phase II trial of 17-allylamino-17-demethoxygeldanamycin in patients with hormone-refractory metastatic prostate cancer. Clin Prostate Cancer 4:138–141
27. Dymock BW, Barril X, Brough PA, Cansfield JE, Massey A, McDonald E, Hubbard RE, Surgenor A, Roughley SD, Webb P, Workman P, Wright L, Drysdale MJ (2005) Novel, potent small-molecule inhibitors of the molecular chaperone Hsp90 discovered through structure-based design. J Med Chem 48:4212–4215
28. Dickey CA, Dunmore J, Lu B, Wang JW, Lee WC, Kamal A, Burrows F, Eckman C, Hutton M, Petrucelli L (2006) HSP induction mediates selective clearance of tau phosphorylated at proline-directed Ser/Thr sites but not KXGS (MARK) sites. FASEB J 20:753–755
29. Avila C, Hadden MK, Ma Z, Kornilayev BA, Ye QZ, Blagg BS (2006) High-throughput screening for Hsp90 ATPase inhibitors. Bioorg Med Chem Lett 16:3005–3008
30. Uehara Y, Hori M, Takeuchi T, Umezawa H (1986) Phenotypic change from transformed to normal induced by benzoquinonoid ansamycins accompanies inactivation of p60src in rat kidney cells infected with Rous sarcoma virus. Mol Cell Biol 6: 2198–2206
31. Whitesell L, Mimnaugh EG, De Costa B, Myers CE, Neckers LM (1994) Inhibition of heat shock protein HSP90–pp60v–src heteroprotein complex formation by benzoquinone ansamycins: essential role for stress proteins in oncogenic transformation. Proc Natl Acad Sci U S A 91:8324–8328
32. Prodromou C, Roe SM, O'Brien R, Ladbury JE, Piper PW, Pearl LH (1997) Identification and structural characterization of the ATP/ADP-binding site in the Hsp90 molecular chaperone. Cell 90:65–75

33. Kamal A, Thao L, Sensintaffar J, Zhang L, Boehm MF, Fritz LC, Burrows FJ (2003) A high-affinity conformation of Hsp90 confers tumour selectivity on Hsp90 inhibitors. Nature 425:407–410
34. Neckers L, Lee YS (2003) Cancer: the rules of attraction. Nature 425:357–359
35. Katsuno M, Adachi H, Kume A, Li M, Nakagomi Y, Niwa H, Sang C, Kobayashi Y, Doyu M, Sobue G (2002) Testosterone reduction prevents phenotypic expression in a transgenic mouse model of spinal and bulbar muscular atrophy. Neuron 35: 843–854
36. Merry DE (2005) Animal models of Kennedy disease. NeuroRx 2:471–479
37. Katsuno M, Adachi H, Doyu M, Minamiyama M, Sang C, Kobayashi Y, Inukai A, Sobue G (2003) Leuprorelin rescues polyglutamine-dependent phenotypes in a transgenic mouse model of spinal and bulbar muscular atrophy. Nat Med 9: 768–773
38. Katsuno M, Adachi H, Tanaka F, Sobue G (2004) Spinal and bulbar muscular atrophy: ligand-dependent pathogenesis and therapeutic perspectives. J Mol Med 82:298–307
39. Katsuno M, Adachi H, Waza M, Banno H, Suzuki K, Tanaka F, Doyu M, Sobue G (2006) Pathogenesis, animal models and therapeutics in Spinal and bulbar muscular atrophy (SBMA). Exp Neurol (In press)
40. Adachi H, Katsuno M, Minamiyama M, Sang C, Pagoulatos G, Angelidis C, Kusakabe M, Yoshiki A, Kobayashi Y, Doyu M, Sobue G (2003) Heat shock protein 70 chaperone overexpression ameliorates phenotypes of the spinal and bulbar muscular atrophy transgenic mouse model by reducing nuclear-localized mutant androgen receptor protein. J Neurosci 23:2203–2211
41. Minamiyama M, Katsuno M, Adachi H, Waza M, Sang C, Kobayashi Y, Tanaka F, Doyu M, Inukai A, Sobue G (2004) Sodium butyrate ameliorates phenotypic expression in a transgenic mouse model of spinal and bulbar muscular atrophy. Hum Mol Genet 13:1183–1192
42. Banno H, Adachi H, Katsuno M, Suzuki K, Atsuta N, Watanabe H, Tanaka F, Doyu M, Sobue G (2006) Mutant androgen receptor accumulation in spinal and bulbar muscular atrophy scrotal skin: a pathogenic marker. Ann Neurol 59: 520–526
43. Sullivan W, Stensgard B, Caucutt G, Bartha B, McMahon N, Alnemri ES, Litwack G, Toft D (1997) Nucleotides and two functional states of hsp90. J Biol Chem 272:8007–8012
44. Egorin MJ, Zuhowski EG, Rosen DM, Sentz DL, Covey JM, Eiseman JL (2001) Plasma pharmacokinetics and tissue distribution of 17-(allylamino)-17-demethoxygeldanamycin (NSC 330507) in CD2F1 mice1. Cancer Chemother Pharmacol 47:291–302
45. McClellan AJ, Scott MD, Frydman J (2005) Folding and quality control of the VHL tumor suppressor proceed through distinct chaperone pathways. Cell 121:739–748
46. Felts SJ, Toft DO (2003) p23, a simple protein with complex activities. Cell Stress Chaperones 8:108–113
47. Mimnaugh EG, Chavany C, Neckers L (1996) Polyubiquitination and proteasomal degradation of the p185c-erbB-2 receptor protein-tyrosine kinase induced by geldanamycin. J Biol Chem 271:22796–22801
48. Bonvini P, Dalla Rosa H, Vignes N, Rosolen A (2004) Ubiquitination and proteasomal degradation of nucleophosmin-anaplastic lymphoma kinase induced by 17-allylamino-demethoxygeldanamycin: role of the co-chaperone carboxyl heat shock protein 70-interacting protein. Cancer Res 64:3256–3264
49. Smith DF, Whitesell L, Nair SC, Chen S, Prapapanich V, Rimerman RA (1995) Progesterone receptor structure and function altered by geldanamycin, an hsp90-binding agent. Mol Cell Biol 15:6804–6812
50. Johnson JL, Toft DO (1995) Binding of p23 and hsp90 during assembly with the progesterone receptor. Mol Endocrinol 9:670–678
51. Whitesell L, Cook P (1996) Stable and specific binding of heat shock protein 90 by geldanamycin disrupts glucocorticoid receptor function in intact cells. Mol Endocrinol 10:705–712
52. Whitesell L, Bagatell R, Falsey R (2003) The stress response: implications for the clinical development of hsp90 inhibitors. Curr Cancer Drug Targets 3:349–358
53. Kamal A, Boehm MF, Burrows FJ (2004) Therapeutic and diagnostic implications of Hsp90 activation. Trends Mol Med 10:283–290
54. Muchowski PJ, Wacker JL (2005) Modulation of neurodegeneration by molecular chaperones. Nat Rev Neurosci 6:11–22
55. Ross CA, Poirier MA (2004) Protein aggregation and neurodegenerative disease. Nat Med 10:10–17 (Suppl)
56. Arrasate M, Mitra S, Schweitzer ES, Segal MR, Finkbeiner S (2004) Inclusion body formation reduces levels of mutant huntingtin and the risk of neuronal death. Nature 431:805–810
57. Sittler A, Lurz R, Lueder G, Priller J, Lehrach H, Hayer-Hartl MK, Hartl FU, Wanker EE (2001) Geldanamycin activates a heat shock response and inhibits huntingtin aggregation in a cell culture model of Huntington's disease. Hum Mol Genet 10:1307–1315
58. Xia H, Mao Q, Eliason SL, Harper SQ, Martins IH, Orr HT, Paulson HL, Yang L, Kotin RM, Davidson BL (2004) RNAi suppresses polyglutamine-induced neurodegeneration in a model of spinocerebellar ataxia. Nat Med 10:816–820
59. Harper SQ, Staber PD, He X, Eliason SL, Martins IH, Mao Q, Yang L, Kotin RM, Paulson HL, Davidson BL (2005) RNA interference improves motor and neuropathological abnormalities in a Huntington's disease mouse model. Proc Natl Acad Sci U S A 102:5820–5825
60. Raoul C, Abbas-Terki T, Bensadoun JC, Guillot S, Haase G, Szulc J, Henderson CE, Aebischer P (2005) Lentiviral-mediated silencing of SOD1 through RNA interference retards disease onset and progression in a mouse model of ALS. Nat Med 11:423–428
61. Bailey CK, Andriola IF, Kampinga HH, Merry DE (2002) Molecular chaperones enhance the degradation of expanded polyglutamine repeat androgen receptor in a cellular model of spinal and bulbar muscular atrophy. Hum Mol Genet 11: 515–523
62. La Spada AR, Weydt P (2005) Targeting toxic proteins for turnover. Nat Med 11:1052–1053
63. Cummings CJ, Mancini MA, Antalffy B, DeFranco DB, Orr HT, Zoghbi HY (1998) Chaperone suppression of aggregation and altered subcellular proteasome localization imply protein misfolding in SCA1. Nat Genet 19:148–154
64. Ciechanover A, Brundin P (2003) The ubiquitin proteasome system in neurodegenerative diseases: sometimes the chicken, sometimes the egg. Neuron 40:427–446
65. Bence NF, Sampat RM, Kopito RR (2001) Impairment of the ubiquitin–proteasome system by protein aggregation. Science 292:1552–1555
66. Jana NR, Zemskov EA, Wang G, Nukina N (2001) Altered proteasomal function due to the expression of polyglutamine-expanded truncated N-terminal huntingtin induces apoptosis by caspase activation through mitochondrial cytochrome *c* release. Hum Mol Genet 10:1049–1059
67. Holmberg CI, Staniszewski KE, Mensah KN, Matouschek A, Morimoto RI (2004) Inefficient degradation of truncated polyglutamine proteins by the proteasome. EMBO J 23: 4307–4318
68. Zhou H, Cao F, Wang Z, Yu ZX, Nguyen HP, Evans J, Li SH, Li XJ (2003) Huntingtin forms toxic NH2-terminal fragment complexes that are promoted by the age-dependent decrease in proteasome activity. J Cell Biol 163:109–118
69. Bowman AB, Yoo SY, Dantuma NP, Zoghbi HY (2005) Neuronal dysfunction in a polyglutamine disease model occurs in the absence of ubiquitin–proteasome system impairment and inversely correlates with the degree of nuclear inclusion formation. Hum Mol Genet 14:679–691

70. Bett JS, Goellner GM, Woodman B, Pratt G, Rechsteiner M, Bates GP (2006) Proteasome impairment does not contribute to pathogenesis in R6/2 Huntington's disease mice: exclusion of proteasome activator REG{gamma} as a therapeutic target. Hum Mol Genet 15:33–44
71. Yamamoto A, Lucas JJ, Hen R (2000) Reversal of neuropathology and motor dysfunction in a conditional model of Huntington's disease. Cell 101:57–66
72. Zu T, Duvick LA, Kaytor MD, Berlinger MS, Zoghbi HY, Clark HB, Orr HT (2004) Recovery from polyglutamine-induced neurodegeneration in conditional SCA1 transgenic mice. J Neurosci 24:8853–8861
73. Chen HK, Fernandez-Funez P, Acevedo SF, Lam YC, Kaytor MD, Fernandez MH, Aitken A, Skoulakis EM, Orr HT, Botas J, Zoghbi HY (2003) Interaction of Akt-phosphorylated ataxin-1 with 14-3-3 mediates neurodegeneration in spinocerebellar ataxia type 1. Cell 113:457–468
74. Koprivica V, Cho KS, Park JB, Yiu G, Atwal J, Gore B, Kim JA, Lin E, Tessier-Lavigne M, Chen DF, He Z (2005) EGFR activation mediates inhibition of axon regeneration by myelin and chondroitin sulfate proteoglycans. Science 310:106–110
75. Herrmann O, Baumann B, de Lorenzi R, Muhammad S, Zhang W, Kleesiek J, Malfertheiner M, Kohrmann M, Potrovita I, Maegele I, Beyer C, Burke JR, Hasan MT, Bujard H, Wirth T, Pasparakis M, Schwaninger M (2005) IKK mediates ischemia-induced neuronal death. Nat Med 11:1322–1329
76. Bagatell R, Paine-Murrieta GD, Taylor CW, Pulcini EJ, Akinaga S, Benjamin IJ, Whitesell L (2000) Induction of a heat shock factor 1-dependent stress response alters the cytotoxic activity of hsp90-binding agents. Clin Cancer Res 6:3312–3318
77. Murakami Y, Uehara Y, Yamamoto C, Fukazawa H, Mizuno S (1991) Induction of hsp 72/73 by herbimycin A, an inhibitor of transformation by tyrosine kinase oncogenes. Exp Cell Res 195:338–344
78. Zou J, Guo Y, Guettouche T, Smith DF, Voellmy R (1998) Repression of heat shock transcription factor HSF1 activation by HSP90 (HSP90 complex) that forms a stress-sensitive complex with HSF1. Cell 94:471–480
79. Rokutan K, Hirakawa T, Teshima S, Nakano Y, Miyoshi M, Kawai T, Konda E, Morinaga H, Nikawa T, Kishi K (1998) Implications of heat shock/stress proteins for medicine and disease. J Med Investig 44:137–147
80. Warrick JM, Chan HY, Gray-Board GL, Chai Y, Paulson HL, Bonini NM (1999) Suppression of polyglutamine-mediated neurodegeneration in *Drosophila* by the molecular chaperone HSP70. Nat Genet 23:425–428
81. Wyttenbach A, Carmichael J, Swartz J, Furlong RA, Narain Y, Rankin J, Rubinsztein DC (2000) Effects of heat shock, heat shock protein 40 (HDJ-2), and proteasome inhibition on protein aggregation in cellular models of Huntington's disease. Proc Natl Acad Sci U S A 97:2898–2903
82. Katsuno M, Sang C, Adachi H, Minamiyama M, Waza M, Tanaka F, Doyu M, Sobue G (2005) Pharmacological induction of heat-shock proteins alleviates polyglutamine-mediated motor neuron disease. Proc Natl Acad Sci U S A 102:16801–16806
83. Hay DG, Sathasivam K, Tobaben S, Stahl B, Marber M, Mestril R, Mahal A, Smith DL, Woodman B, Bates GP (2004) Progressive decrease in chaperone protein levels in a mouse model of Huntington's disease and induction of stress proteins as a therapeutic approach. Hum Mol Genet 13:1389–1405
84. Agrawal N, Pallos J, Slepko N, Apostol BL, Bodai L, Chang LW, Chiang AS, Thompson LM, Marsh JL (2005) Identification of combinatorial drug regimens for treatment of Huntington's disease using *Drosophila*. Proc Natl Acad Sci U S A 102:3777–3781
85. Dou F, Netzer WJ, Tanemura K, Li F, Hartl FU, Takashima A, Gouras GK, Greengard P, Xu H (2003) Chaperones increase association of tau protein with microtubules. Proc Natl Acad Sci U S A 100:721–726
86. Petrucelli L, Dickson D, Kehoe K, Taylor J, Snyder H, Grover A, De Lucia M, McGowan E, Lewis J, Prihar G, Kim J, Dillmann WH, Browne SE, Hall A, Voellmy R, Tsuboi Y, Dawson TM, Wolozin B, Hardy J, Hutton M (2004) CHIP and Hsp70 regulate tau ubiquitination, degradation and aggregation. Hum Mol Genet 13:703–714
87. Benussi L, Ghidoni R, Paterlini A, Nicosia F, Alberici AC, Signorini S, Barbiero L, Binetti G (2005) Interaction between tau and alpha-synuclein proteins is impaired in the presence of P301L tau mutation. Exp Cell Res 308:78–84
88. Auluck PK, Bonini NM (2002) Pharmacological prevention of Parkinson disease in *Drosophila*. Nat Med 8:1185–1186
89. Auluck PK, Meulener MC, Bonini NM (2005) Mechanisms of suppression of {alpha}-synuclein neurotoxicity by geldanamycin in *Drosophila*. J Biol Chem 280:2873–2878
90. Flower TR, Chesnokova LS, Froelich CA, Dixon C, Witt SN (2005) Heat shock prevents alpha-synuclein-induced apoptosis in a yeast model of Parkinson's disease. J Mol Biol 351: 1081–1100
91. Lu A, Ran R, Parmentier-Batteur S, Nee A, Sharp FR (2002) Geldanamycin induces heat shock proteins in brain and protects against focal cerebral ischemia. J Neurochem 81:355–364
92. Giffard RG, Xu L, Zhao H, Carrico W, Ouyang Y, Qiao Y, Sapolsky R, Steinberg G, Hu B, Yenari MA (2004) Chaperones, protein aggregation, and brain protection from hypoxic/ischemic injury. J Exp Biol 207:3213–3220
93. Murphy P, Sharp A, Shin J, Gavrilyuk V, Dello Russo C, Weinberg G, Sharp FR, Lu A, Heneka MT, Feinstein DL (2002) Suppressive effects of ansamycins on inducible nitric oxide synthase expression and the development of experimental autoimmune encephalomyelitis. J Neurosci Res 67:461–470
94. Xiao N, Callaway CW, Lipinski CA, Hicks SD, DeFranco DB (1999) Geldanamycin provides posttreatment protection against glutamate-induced oxidative toxicity in a mouse hippocampal cell line. J Neurochem 72:95–101
95. Sano M (2001) Radicicol and geldanamycin prevent neurotoxic effects of anti-cancer drugs on cultured embryonic sensory neurons. Neuropharmacology 40:947–953
96. Xu L, Ouyang YB, Giffard RG (2003) Geldanamycin reduces necrotic and apoptotic injury due to oxygen-glucose deprivation in astrocytes. Neurol Res 25:697–700
97. Ouyang YB, Xu L, Giffard RG (2005) Geldanamycin treatment reduces delayed CA1 damage in mouse hippocampal organotypic cultures subjected to oxygen glucose deprivation. Neurosci Lett 380:229–233
98. Dou F, Yuan LD, Zhu JJ (2005) Heat shock protein 90 indirectly regulates ERK activity by affecting Raf protein metabolism. Acta Biochim Biophys Sin (Shanghai) 37: 501–505
99. Stancato LF, Chow YH, Hutchison KA, Perdew GH, Jove R, Pratt WB (1993) Raf exists in a native heterocomplex with hsp90 and p50 that can be reconstituted in a cell-free system. J Biol Chem 268:21711–21716
100. Ferrer I, Blanco R, Carmona M, Ribera R, Goutan E, Puig B, Rey MJ, Cardozo A, Vinals F, Ribalta T (2001) Phosphorylated map kinase (ERK1, ERK2) expression is associated with early tau deposition in neurones and glial cells, but not with increased nuclear DNA vulnerability and cell death, in Alzheimer disease, Pick's disease, progressive supranuclear palsy and corticobasal degeneration. Brain Pathol 11:144–158
101. Pei JJ, Braak H, An WL, Winblad B, Cowburn RF, Iqbal K, Grundke-Iqbal I (2002) Up-regulation of mitogen-activated protein kinases ERK1/2 and MEK1/2 is associated with the progression of neurofibrillary degeneration in Alzheimer's disease. Brain Res Mol Brain Res 109:45–55
102. LaFevre-Bernt MA, Ellerby LM (2003) Kennedy's disease. Phosphorylation of the polyglutamine-expanded form of androgen receptor regulates its cleavage by caspase-3 and enhances cell death. J Biol Chem 278:34918–34924

103. Murray B, Alessandrini A, Cole AJ, Yee AG, Furshpan EJ (1998) Inhibition of the p44/42 MAP kinase pathway protects hippocampal neurons in a cell-culture model of seizure activity. Proc Natl Acad Sci U S A 95:11975–11980
104. Cheung EC, Slack RS (2004) Emerging role for ERK as a key regulator of neuronal apoptosis. Sci STKE 2004:PE45
105. Subramaniam S, Zirrgiebel U, von Bohlen Und Halbach O, Strelau J, Laliberte C, Kaplan DR, Unsicker K (2004) ERK activation promotes neuronal degeneration predominantly through plasma membrane damage and independently of caspase-3. J Cell Biol 165:357–369
106. Zhu X, Lee HG, Raina AK, Perry G, Smith MA (2002) The role of mitogen-activated protein kinase pathways in Alzheimer's disease. NeuroSignals 11:270–281
107. Kaytor MD, Byam CE, Tousey SK, Stevens SD, Zoghbi HY, Orr HT (2005) A cell-based screen for modulators of ataxin-1 phosphorylation. Hum Mol Genet 14:1095–1105
108. Sato S, Fujita N, Tsuruo T (2000) Modulation of Akt kinase activity by binding to Hsp90. Proc Natl Acad Sci U S A 97:10832–10837
109. George P, Bali P, Cohen P, Tao J, Guo F, Sigua C, Vishvanath A, Fiskus W, Scuto A, Annavarapu S, Moscinski L, Bhalla K (2004) Cotreatment with 17-allylamino-demethoxygeldanamycin and FLT-3 kinase inhibitor PKC412 is highly effective against human acute myelogenous leukemia cells with mutant FLT-3. Cancer Res 64:3645–3652
110. Datta SR, Brunet A, Greenberg ME (1999) Cellular survival: a play in three Akts. Genes Dev 13:2905–2927
111. Pai KS, Cunningham DD (2002) Geldanamycin specifically modulates thrombin-mediated morphological changes in mouse neuroblasts. J Neurochem 80:715–718
112. Xu W, Marcu M, Yuan X, Mimnaugh E, Patterson C, Neckers L (2002) Chaperone-dependent E3 ubiquitin ligase CHIP mediates a degradative pathway for c-ErbB2/Neu. Proc Natl Acad Sci U S A 99:12847–12852
113. Lavictoire SJ, Parolin DA, Klimowicz AC, Kelly JF, Lorimer IA (2003) Interaction of Hsp90 with the nascent form of the mutant epidermal growth factor receptor EGFRvIII. J Biol Chem 278:5292–5299
114. Chen G, Cao P, Goeddel DV (2002) TNF-induced recruitment and activation of the IKK complex require Cdc37 and Hsp90. Mol Cell 9:401–410
115. Luedde T, Assmus U, Wustefeld T, Meyer zu Vilsendorf A, Roskams T, Schmidt-Supprian M, Rajewsky K, Brenner DA, Manns MP, Pasparakis M, Trautwein C (2005) Deletion of IKK2 in hepatocytes does not sensitize these cells to TNF-induced apoptosis but protects from ischemia/reperfusion injury. J Clin Invest 115:849–859
116. Apostol BL, Illes K, Pallos J, Bodai L, Wu J, Strand A, Schweitzer ES, Olson JM, Kazantsev A, Marsh JL, Thompson LM (2006) Mutant huntingtin alters MAPK signaling pathways in PC12 and striatal cells: ERK1/2 protects against mutant huntingtin-associated toxicity. Hum Mol Genet 15:273–285
117. Song C, Perides G, Liu YF (2002) Expression of full-length polyglutamine-expanded Huntingtin disrupts growth factor receptor signaling in rat pheochromocytoma (PC12) cells. J Biol Chem 277:6703–6707
118. Lievens JC, Rival T, Iche M, Chneiweiss H, Birman S (2005) Expanded polyglutamine peptides disrupt EGF receptor signaling and glutamate transporter expression in *Drosophila*. Hum Mol Genet 14:713–724
119. Levy Y, Gorshtein A (2005) Chaperones and disease. N Engl J Med 353:2821–2822
120. Pearl LH, Prodromou C (2001) Structure, function, and mechanism of the Hsp90 molecular chaperone. Adv Protein Chem 59:157–186

THE JOURNAL OF BIOLOGICAL CHEMISTRY VOL. 281, NO. 33, pp. 23842–23851, August 18, 2006

Archaeal Proteasomes Effectively Degrade Aggregation-prone Proteins and Reduce Cellular Toxicities in Mammalian Cells*

Received for publication, February 9, 2006, and in revised form, May 25, 2006 Published, JBC Papers in Press, June 22, 2006, DOI 10.1074/jbc.M601274200

Shin-ichi Yamada, Jun-ichi Niwa, Shinsuke Ishigaki, Miho Takahashi, Takashi Ito, Jun Sone, Manabu Doyu, and Gen Sobue[1]

From the Department of Neurology, Nagoya University Graduate School of Medicine, 65 Tsurumai-cho, Showa-ku, Nagoya-city, Aichi 466-8550, Japan

The 20 S proteasome is a ubiquitous, barrel-shaped protease complex responsible for most of cellular proteolysis, and its reduced activity is thought to be associated with accumulations of aberrant or misfolded proteins, resulting in a number of neurodegenerative diseases, including amyotrophic lateral sclerosis, spinal and bulbar muscular atrophy, Parkinson disease, and Alzheimer disease. The 20 S proteasomes of archaebacteria (archaea) are structurally simple and proteolytically powerful and thought to be an evolutionary precursor to eukaryotic proteasomes. We successfully reproduced the archaeal proteasome in a functional state in mammalian cells, and here we show that the archaeal proteasome effectively accelerated species-specific degradation of mutant superoxide dismutase-1 and the mutant polyglutamine tract-extended androgen receptor, causative proteins of familial amyotrophic lateral sclerosis and spinal and bulbar muscular atrophy, respectively, and reduced the cellular toxicities of these mutant proteins. Further, we demonstrate that archaeal proteasome can also degrade other neurodegenerative disease-associated proteins such as α-synuclein and tau. Our study showed that archaeal proteasomes can degrade aggregation-prone proteins whose toxic gain of function causes neurodegradation and reduce protein cellular toxicity.

The 20 S proteasome is a ubiquitous, barrel-shaped protease complex responsible for most of cellular proteolysis (1) and is formed by four stacked seven-membered rings (2). The α-type subunits, which are proteolytically inactive (3), form the outer rings, and the β-type subunits, which contain the active site (4), form the inner rings of the complex (5). The 20 S proteasome of archaebacteria (archaea) consists of only one type of each of the α- and β-subunits and is thought to be the evolutionary ancestor of the eukaryotic proteasome (6), which is quite similar in architecture to that of archaea but is composed of seven different α- and seven different β-subunits (6). Archaea do not have the ubiquitin recognition system for protein degradation and are thought to have unidentified tags in its degradation pathway (7). Like eukaryotic cells, archaea also have a regulatory complex for the 20 S proteasome, known as proteasome-activating nucleotidase (PAN)[2] (8). PAN is an evolutionary precursor to the 19 S base in eukaryotic cells and thought to be necessary for efficient archaeal 20 S proteasomal protein degradation (8). However *in vitro*, the archaeal 20 S proteasome has been reported to rapidly degrade polyglutamine aggregates without the help of PAN (9). This PAN-independent degradation by the archaeal 20 S proteasome inspired us to introduce and test a novel proteolytic facility in mammalian cells. We have chosen the archaeal *Methanosarcina mazei* (Mm) 20 S proteasome, because its optimal growth temperature is around 37 °C, making it suitable to examine its proteasomal effects in mammalian cells.

The eukaryotic ubiquitin-proteasome system degrades aberrant or misfolded proteins that could otherwise form potentially toxic aggregates (10). These aggregate formations in cells are related to the pathogenesis of several common aging-related neurodegenerative diseases, including Parkinson disease (PD), amyotrophic lateral sclerosis (ALS), polyglutamine diseases (*e.g.* Huntington disease, some spinocerebellar ataxias, and spinal and bulbar muscular atrophy), and Alzheimer disease (AD), which are thought to be associated with the reduced activities of the proteasome (11–15). However, a critical cause of the accumulation of abnormal proteins remains unclear. Solving this common aspect of many neurodegenerative disorders would be a breakthrough in treating these diseases.

In the present study, we show that the Mm proteasome functions in mammalian cells to accelerate the degradation of the following aggregation-prone proteins: mutant superoxide dismutase-1 (SOD1), a causative protein of familial ALS; mutant androgen receptor (AR) with expanded polyglutamine tract, a causative protein of spinal and bulbar muscular atrophy; α-synuclein, an accumulated protein in PD; and tau, an accumulated protein in AD.

* This work was supported by a Center of Excellence grant from the Ministry of Education, Culture, Sports, Science, and Technology of Japan. The costs of publication of this article were defrayed in part by the payment of page charges. This article must therefore be hereby marked "*advertisement*" in accordance with 18 U.S.C. Section 1734 solely to indicate this fact.

[1] To whom correspondence should be addressed. Tel.: 81-52-744-2385; Fax: 81-52-744-2384; E-mail: sobueg@med.nagoya-u.ac.jp.

[2] The abbreviations used are: PAN, proteasome-activating nucleotidase; SOD1, superoxide dismutase-1; Mm, *M. mazei*; ALS, amyotrophic lateral sclerosis; AR, androgen receptor; PD, Parkinson disease; AD, Alzheimer disease; MTS, 3-(4,5-dimethylthiazol-2-yl)-5-(3-carboxymethoxyphenyl)-2-(4-sulfophenyl)-2H-tetrazolium; WT, wild type; NTA, nitrilotriacetic acid; GFP, green fluorescent protein.

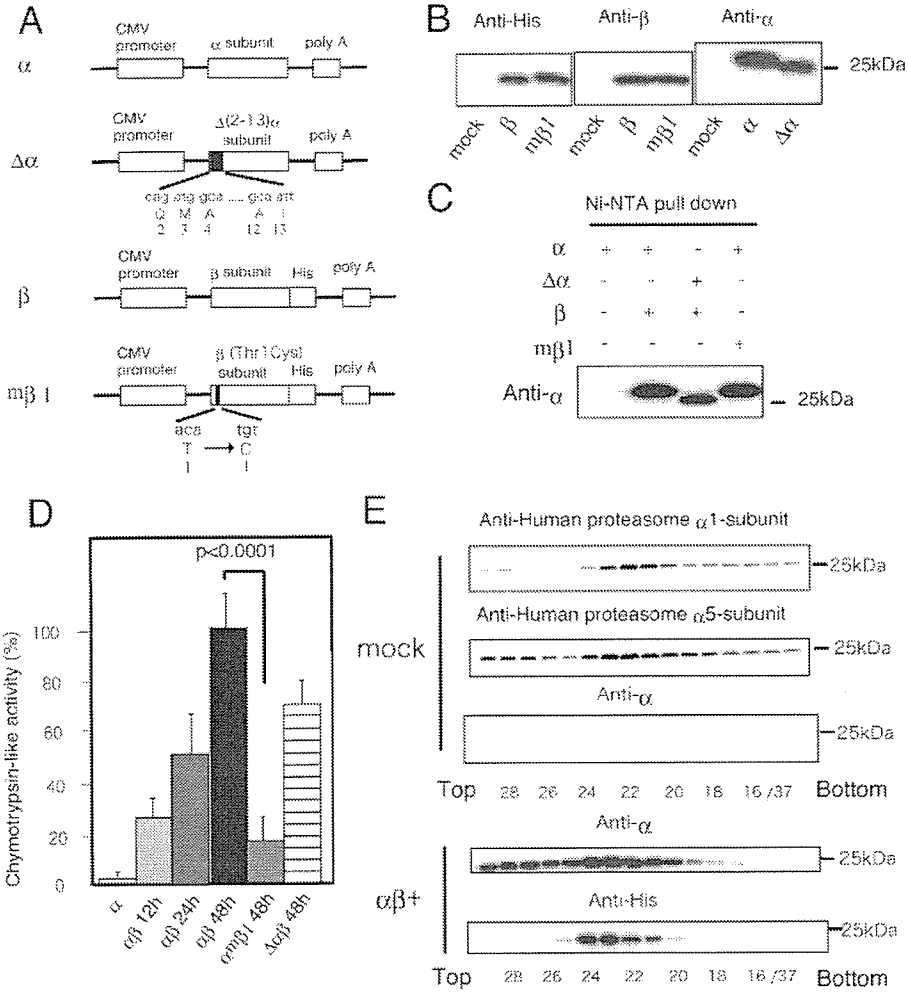

FIGURE 1. **Expression of *M. mazei* proteasome in mammalian cells.** *A*, schematic illustration of expression vectors used in this study. The deleted sequences of the Δα-subunit are depicted. The T1C β-subunit (mβ1) has three mutated base pairs (a to t, c to g, and a to t). *B*, Western blot analysis with anti-proteasome α-subunit, anti-proteasome β-subunit, and anti-His antibodies. *C*, Ni^{2+}-NTA pulldown assay. Pulled down proteins run on SDS-PAGE were probed with anti-proteasome α-subunit. *D*, chymotrypsin-like activity of the Ni^{2+}-NTA pulled down samples. This protease activity gradually became higher after transfection. *Error bars*, S.D. (n = 3). *E*, glycerol gradient centrifugation experiment: Mm proteasome α- and β-subunits fractionated into nearly the same fractions as did the human 20 S proteasome subunits α1 and α5, αβ− and αβ+, indicating that cells were transfected with mock and Mm proteasome αβ, respectively.

EXPERIMENTAL PROCEDURES

Construction of the Expression Vectors: M. mazei Proteasome Subunits α, β, ΔN(2–13)α, and Mutant β (T1C)—The DNA fragment encoding the α-subunit protein (GenBank™ accession number 1480962) was amplified by PCR from the genomic DNA of *M. mazei* (ATCC) using the following primers: αF (5′-GCGGGTACCCCACCATGCAGATGGCACCACAGATG) and αR (5′-CGCCTCGAGTTATTCTTTGTTCTCATTTCCTTTGTG). The Δ(2–13) α-subunit (Δα) was amplified using the following primers: ΔαF (5′-GCGGGTACCCCACCATGACGGTTTTCAGCCCTGACGG) and αR. The amplified fragments were inserted into the KpnI and XhoI site of the pcDNA 3.1(+) vector (Invitrogen). The β-subunit (GenBank™ accession number 1479036) was amplified by PCR with the following primers: βF (5′-GCCTCTAGACCACCATGGATAATGACAAATATTTAAAG) and βR (5′-GCGACCGGTGTTTCCTAAAGCTCTTCTG) and inserted into the XbaI and AgeI site of the pcDNA3.1(+)/MycHis vector (Invitrogen) to fuse it to a His_6 tag. The mutated mβ1-subunit (T1C β-subunit) was generated with a site-directed mutagenesis kit (Stratagene) following the manufacturer's protocol. Construction of pcDNA3.1/MycHis-SOD1 and pCMV-Tag4-SOD1 vectors (WT, G93A, G85R, H46R, and G37R) (16), pEGFP-N1-SOD1 (WT and G93A) vectors, pCR3.1-AR24Q and pCR3.1-AR97Q vectors, and pcDNA3.1(+)/MycHis-α-synuclein (WT, A53T, and A30P) was described previously (16–18). Six isoforms of tau were amplified by PCR from the pRK172 vectors that were kindly provided by Dr. Michel Goedert and inserted into the KpnI and XbaI site of the pcDNA3.1 vector (Invitrogen).

Cell Culture, Transfection, and Antibodies—Neuro2a cells and human embryonic kidney 293 (HEK293) cells were maintained in Dulbecco's modified Eagle's medium with 10% fetal calf serum. Transfections were performed using Lipofectamine 2000 (Invitrogen) in the 3-(4,5-dimethylthiazol-2-yl)-5-(3-carboxymethoxyphenyl)-2-(4-sulfophenyl)-2H-tetrazolium (MTS) assay or Effectene transfection reagent (Qiagen) in other experiments. Antibodies used here were as follows: anti-SOD1 antibody (SOD100; Stressgen Bioreagents), anti-His antibody (Ab-1; Oncogene), anti-α-tubulin antibody (clone B-5-1-1; Sigma), anti-20 S proteasome β-subunit antibody (from *Methanosarcina thermophila*; Calbiochem), anti-20 S proteasome α-subunit antibody (from *M. thermophila*; Calbiochem), anti-AR antibody (N-20; Santa Cruz Biotechnology, Inc., Santa Cruz, CA), anti-α-synuclein antibody (LB509; Zymed Laboratories Inc.), and anti-tau antibody (Mouse Tau-1; Chemicon International).

Glycerol Density Gradient Centrifugation—Cells grown on a 10-cm dish were lysed in 1 ml of 0.01 M Tris-EDTA, pH 7.5, by two freeze-thaw cycles, and the lysates were centrifuged for 15 min at 15 000 × *g* at 4 °C. The cleared supernatants were loaded on the top of a 36-ml linear gradient of glycerol (10–40%) prepared in 25 mM Tris-HCl buffer, pH 7.5, containing 1 mM dithiothreitol and then centrifuged at 80,000 × *g* for 22 h at 4 °C in a Beckman SW28 rotor (Beckman Coulter Inc.). Following centrifugation, 37 fractions (1.0 ml each) were collected from the top of the tubes with a liquid layer injector fractionator (model number CHD255AA; Advantech) connected to a fraction col-

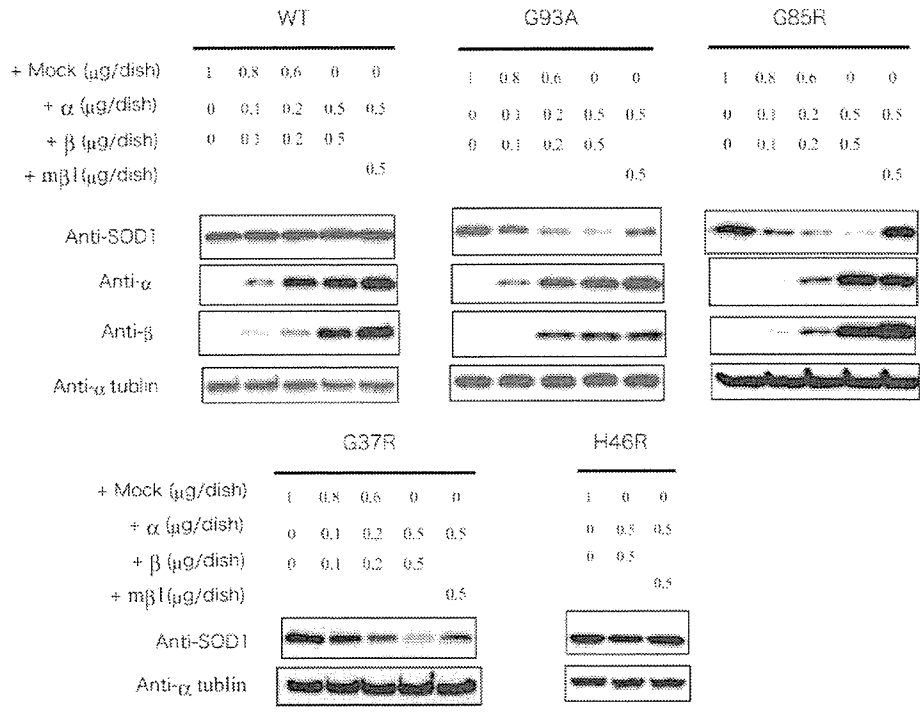

FIGURE 2. **Reduced expression levels of mutant SOD1 proteins in the presence of *M. mazei* proteasome.** Neuro2a cells grown on 6-cm dishes and co-transfected with 1 μg of SOD1-MycHis vector and increasing doses of Mm proteasome subunits were harvested and analyzed 48 h after transfection. The levels of mutant SOD1 proteins were gradually reduced as Mm proteasome αβ increased, whereas no changes in SOD1 proteins were seen with Mm proteasome αmβ1. *WT*, wild-type SOD1; *G93A*, SOD1^{G93A}; *G85R*, SOD1^{G85R}; *G37R*, SOD1^{G37R}; *H46R*, SOD1^{H46R}.

lector. 200 μl of each fraction was precipitated with acetone; the pellets were lysed with 50 μl of sample buffer and then used for SDS-PAGE followed by Western blotting. The immunostained bands were quantified using ImageGauge software (Fuji Film).

Ni^{2+}-NTA Pulldown—HEK 293 cells grown on 10-cm dishes, transfected with Mm proteasome α (as a control), αβ, Δαβ, and αmβ1, were lysed by two freeze-thaw cycles in 1 ml of phosphate-buffered saline buffer and centrifuged at 3000 × *g*. Proteasome complexes were pulled down from the supernatants with 200 μl of Ni^{2+}-NTA-agarose, washed 4 times in 4 ml of 10 mM imidazole/phosphate-buffered saline buffer, and eluted in 2 ml of 250 mM imidazole/phosphate-buffered saline buffer. Samples were then boiled and subjected to Western blotting.

Measurement of the Proteasome Activity—HEK 293 cells grown on 10-cm dishes were transfected with Mm proteasome α (as a control), αβ, Δαβ, and αmβ1. 12, 24, and 48 h after transfection, the cells were lysed and pulled down with Ni^{2+}-NTA. The chymotrypsin-like activity of 500 μl of the Ni^{2+}-NTA pulled down samples were assayed colorimetrically after 12-h incubations at 37 °C with 100 mM Suc-LLVY-amino-4-methylcoumarin (Sigma) by a multiple-plate reader (PowerscanHT, Dainippon Pharmaceutical). The assay was carried out in triplicate and statistically analyzed by one-way analysis of variance.

Immunocytochemistry—Neuro2a cells grown on glass coverslips were co-transfected with pEGFP-N1-SOD1 and Mm proteasome α- and His-tagged β-subunit. 48 h after transfection, cells were fixed, blocked, and incubated with anti-His antibody overnight at 4 °C. After washing, samples were incubated with Alexa-546-conjugated anti-mouse antibody (Molecular Probes, Inc.) and visualized with an Olympus BX51 epifluorescence microscope.

Cycloheximide Chase Analysis—Neuro2a cells grown on 6-cm dishes were transfected with 1 μg of pcDNA3.1/MycHis-SOD1 with mock (0.6 μg), Mm proteasome αmβ1 (0.3 μg each), or Mm proteasome αβ (0.3 μg each). 24 h after transfection, cycloheximide (50 μg/ml) was added to the culture medium, and the cells were harvested at the indicated time points. The samples were subjected to SDS-PAGE and analyzed by Western blotting with anti-SOD1 antibody.

Pulse-chase Analysis—Neuro2a cells grown on 6-cm dishes were transfected with 1 μg of pCMV-Tag4-SOD1^{G93A} with mock (0.6 μg) Mm proteasome αmβ1 (0.3 μg each) or Mm proteasome αβ (0.3 μg each). 24 h after transfection, cells were pulse-labeled with [^{35}S]Cys for 60 min and harvested at the indicated time points. After the immunoprecipitation by anti-FLAG antibody (M2; Sigma), the samples were subjected to SDS-PAGE, phosphor-imaged (Typhoon 9410; Genaral Electric Co.), and statistically analyzed by one-way analysis of variance.

Cell Viability Analysis—HEK293 cells were grown on collagen-coated 96-well plates and co-transfected with pcDNA3.1/MycHis-SOD1 (WT, G93A, and G85R) and Mm 20 S proteasome αβ, αmβ1, or mock in 12 wells each. The MTS-based cell proliferation assays were performed after 48 h of transfection. Absorbance at 490 nm was measured at 37 °C in a multiple-plate reader (PowerscanHT, Dainippon Pharmaceutical). The assay was carried out in triplicate and statistically analyzed by one-way analysis of variance.

Caspase-3/7 Assay—HEK293 cells were grown on black 96-well plates and co-transfected with pcDNA3.1/MycHis-SOD1 (WT, G93A, and G85R) and Mm 20 S proteasome αβ, αmβ1, or mock. 24 h after transfection, the medium was replaced with serum-free medium (Dulbecco's modified Eagle's medium). After 24 h, activated caspase-3/7 activity was analyzed by the Apo-ONE homogeneous caspase-3/7 assay (Promega) following the manufacturer's instructions.

RESULTS

Cloning and Expression of M. mazei Proteasome—We cloned the Mm proteasome α-subunit (GenBank™ accession number 1480962) and β-subunit (GenBank™ accession number 1479036) from genomic DNA of Mm (Fig. 1*A*) and generated a mutant α-subunit lacking amino acids 2–13, Δ(2–13) α-subunit (Δα) (Fig. 1*A*). These amino acids (positions 2–13) nor-

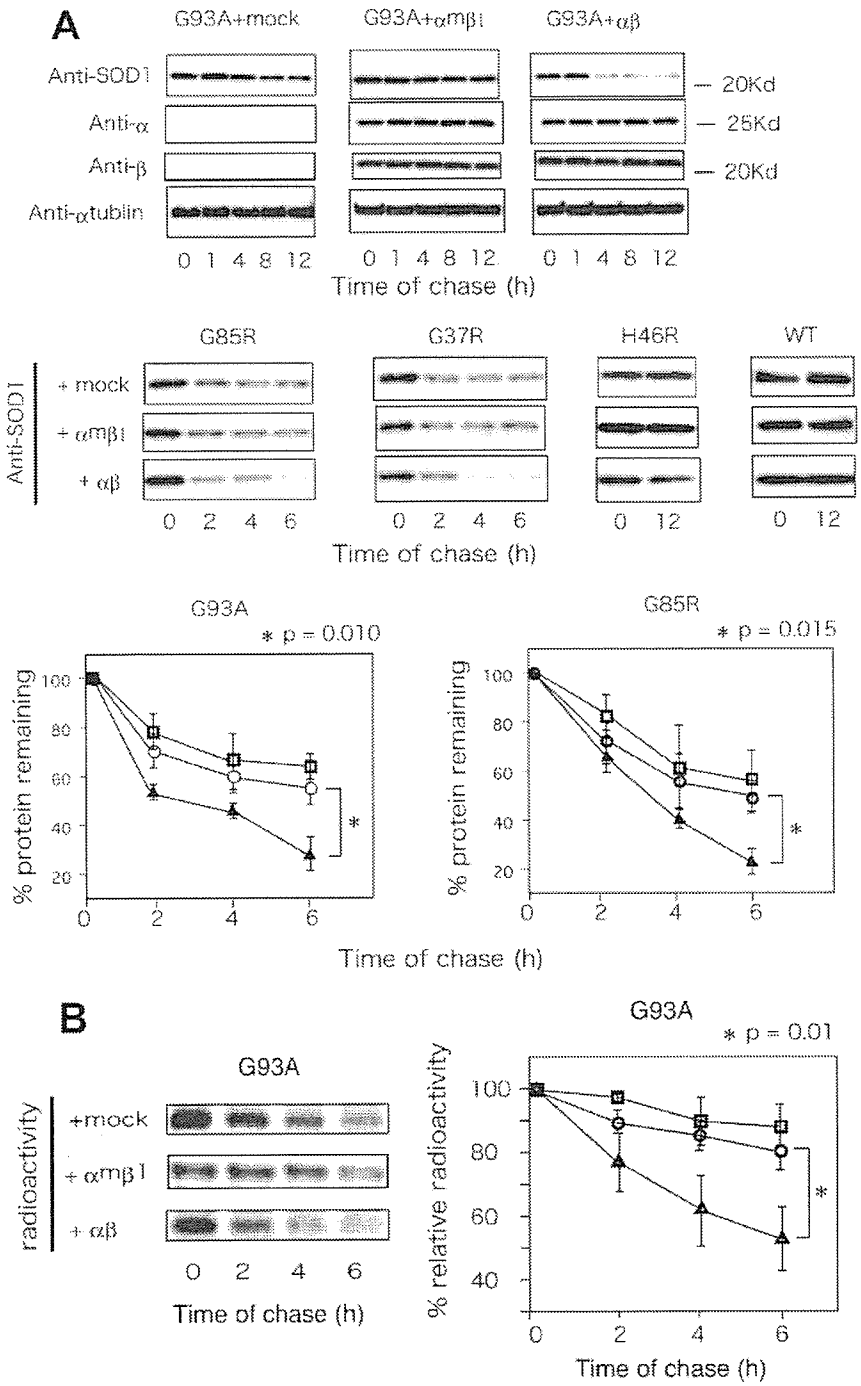

FIGURE 3. ***M. mazei* proteasome-accelerated degradation of mutant SOD1 proteins.** *A*, cycloheximide chase analysis (see "Experimental Procedures") showing that the half-lives of various mutant SOD1 proteins were reduced in the presence of Mm 20 S proteasome $\alpha\beta$. The *graphs* represent the percentage of degraded $SOD1^{G93A}$ and $SOD1^{G85R}$ proteins in three independent experiments. The *error bars* indicate S.D. *B*, pulse-chase analysis (see "Experimental Procedures") showing that the degradation of $SOD1^{G93A}$ was accelerated in the presence of Mm 20 S proteasome $\alpha\beta$. *Circle*, mock; *triangle*, $\alpha\beta$; *square*, $\alpha m\beta 1$. *Error bars*, S.D. ($n = 3$).

mally form a gated channel in the α-ring that regulates substrate entry into the 20 S proteasome (19). We also generated a mutant β-subunit with T1C ($m\beta 1$) (Fig. 1*A*). Thr-1 in the β-subunit of the archaeal proteasome is essential for proteolysis, and Thr-1 mutants lose their proteolytic activities (20). The following experiments were performed in both HEK293 and Neuro2a cells with similar results in both cell lines.

To confirm protein expression of the Mm subunits, HEK293 cells transfected with mock, α, $\Delta\alpha$, β, or $m\beta 1$ were lysed, subjected to SDS-PAGE, and immunoblotted with anti-proteasome α-subunit, anti-proteasome β-subunit, and anti-His antibodies. Fig. 1*B* demonstrates that the α- and β-subunit antibodies detected the Mm proteasome α-subunit at 26 kDa, the $\Delta\alpha$-subunit around 25 kDa, and the β-subunit at 22 kDa, respectively, and faintly recognized endogenous human proteasome subunits. A Ni^{2+}-NTA pull-down assay showed that the Mm proteasome α- and $\Delta\alpha$-subunits co-sedimented with the Mm proteasome β- and $m\beta 1$-subunits but not with mock (Fig. 1*C*), and protease activity of the pulled down samples of the cells lysed 48 h after transfection showed significantly higher chymotrypsin-like protease activity in the Mm proteasome $\alpha\beta$ than in the $\alpha m\beta 1$ or mock-transfected samples (Fig. 1*D*). This protease activity was confirmed to become gradually higher after transfection (Fig. 1*D*).

Glycerol density gradient centrifugation fractionated the $\alpha\beta$, $\Delta\alpha\beta$, and $\alpha m\beta 1$ complexes of the Mm proteasome into nearly the same fractions as those of the human 20 S proteasome subunits $\alpha 1$ and $\alpha 5$ (Fig. 1*E*, data not shown for $\Delta\alpha\beta$ and $\alpha m\beta 1$). Moreover, of the anti-His-immunoblotted bands (Fig. 1*E*), the density of staining in fractions 20–25 accounts for about 80–90% of the total anti-His staining. That these fractions constitute the majority of the anti-α staining as well suggests that about 80–90% of the β-subunit expression is incorporated into the Mm proteasome. These results suggested that the Mm proteasome α-, $\Delta\alpha$-, β-, and $m\beta 1$-subunits could properly assemble to form four stacked seven-membered rings and that an active Mm proteasome could be reproduced in mammalian cells. The cells expressing Mm proteasome $\Delta\alpha\beta$ displayed cellular toxicity, whereas the cells expressing Mm proteasome $\alpha\beta$ showed little toxicity

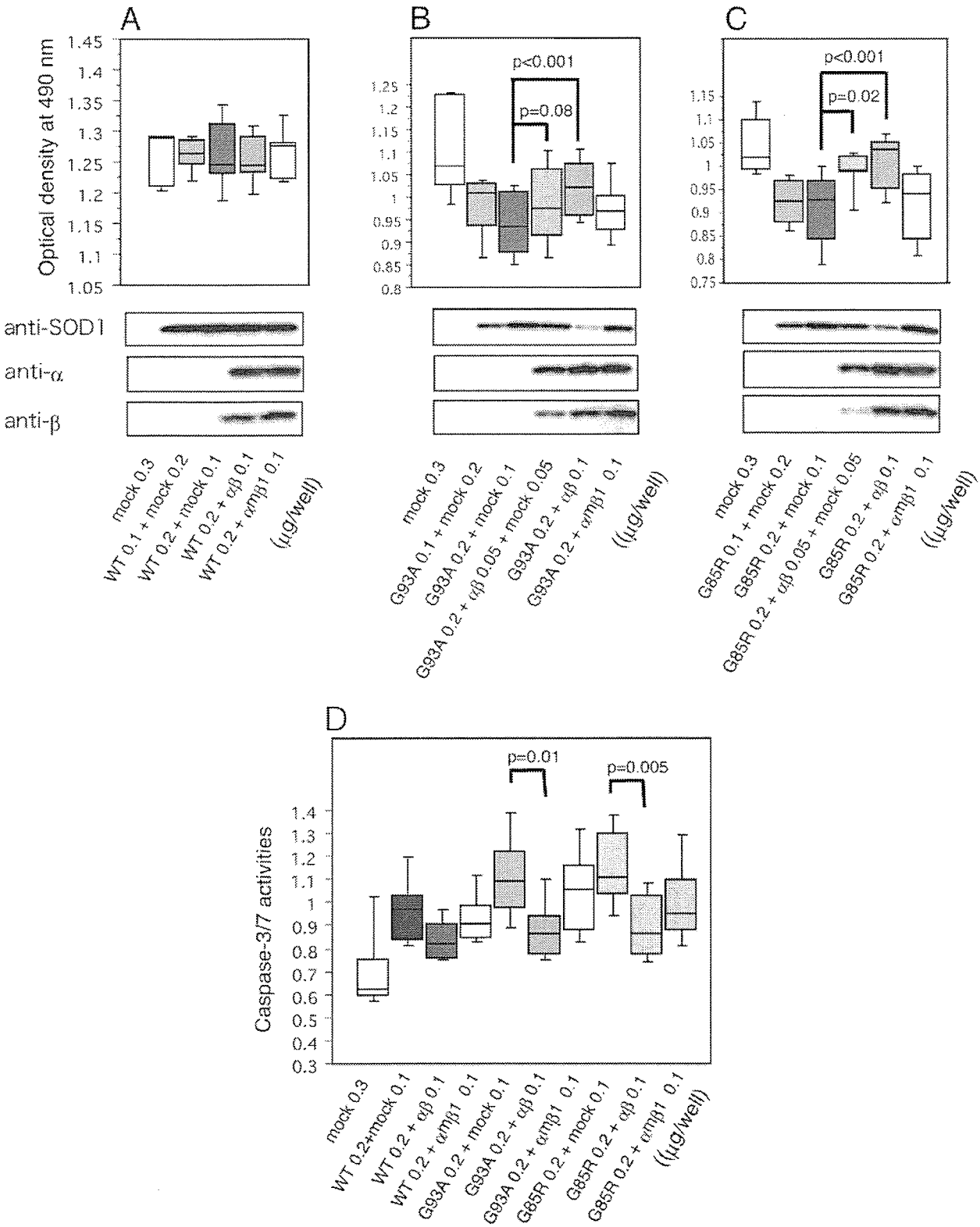

FIGURE 4. ***M. mazei* proteasome reduces the cellular toxicity of mutant SOD1.** The dose-dependent rescue effect of Mm proteasome $\alpha\beta$ expression on cell viability in $SOD1^{WT}$- (*A*), $SOD1^{G93A}$- (*B*), and $SOD1^{G85R}$-transfected HEK293 cells (*C*) as shown in MTS-based cell proliferation assays. The *box plots* show the median values (*center line* of *box*), the 25th (*lower line* of *box*), 75th (*upper line* of *box*), 10th (*lower T bar*), and 90th (*upper T bar*) percentiles in each group ($n = 3 \times 6$ wells). The *numbers* indicate the dose of DNA transfected in each well of a 96-well plate ($\alpha\beta$, 0.1 μg; α, 0.05 μg; β, 0.05 μg). The expression levels of SOD1, α-subunit, and β-subunit at the analyzed points are shown. *D*, relative activities of cleaved caspase-3/7 were analyzed with the fluorescent caspase substrate, benzyloxycarbonyl-DEVD-R110. Production of Mm proteasome $\alpha\beta$ prevents activation of caspase-3/7. Positive control value was 3.2 ± 0.2 (S.D.) ($n = 3 \times 4$ wells) (1 μM staurosporin, 24 h).

(data not shown); thus, further experiments were carried out with Mm proteasomes $\alpha\beta$ and $\alpha m\beta 1$.

M. mazei Proteasome Degrades Specifically Mutant Superoxide Dismutase-1—We then assessed whether the Mm proteasome actually affects mutant SOD1 protein ($SOD1^{G85R}$, $SOD1^{G37R}$, $SOD1^{G93A}$, and $SOD1^{H46R}$) expression. In cultured cells, mutant $SOD1^{G85R}$, $SOD1^{G37R}$, and $SOD1^{G93A}$ are more likely to form aggregates than is $SOD1^{H46R}$ (16), and cases of familial ALS expressing these mutant forms are also more severe than those expressing $SOD1^{H46R}$. Western blot analyses demonstrated that the levels of mutant SOD1 were markedly reduced as the expression of Mm proteasome $\alpha\beta$ increased (Fig. 2). However, wild-type SOD1 levels were not affected by the expression of Mm proteasome $\alpha\beta$. Furthermore, mutant SOD1 levels were not affected by the expression of Mm proteasome containing the $m\beta 1$-subunit in all mutant species, indicating that Mm proteasomal activity was important to reduce the levels of mutant SOD1 proteins. That the expression level of $SOD1^{H46R}$ was less affected by Mm proteasomal expression than other mutant SOD1 species may be associated with the lower toxicity of $SOD1^{H46R}$.

To determine whether the reduced levels of mutant SOD1 protein were due to accelerated degradation of mutant SOD1 or to the reduction of mutant SOD1 expression, we examined the stability of mutant SOD1 proteins expressed in Neuro2a cells co-expressed with Mm proteasome $\alpha\beta$, $\alpha m\beta 1$, or mock (Fig. 3, *A* and *B*). Chase experiments with cycloheximide, which halts all cellular protein synthesis, demonstrated mutant species-dependent acceleration in SOD1 protein degradation, whereas the expression levels of Mm proteasome α- and β-subunits did not change (Fig. 3*A*). The degree of wild-type SOD1 degradation was not affected by the expression of Mm proteasome $\alpha\beta$. Pulse-chase experiments further confirmed that ^{35}S-labeled $SOD1^{G93A}$ degradation was significantly accelerated when co-expressed with Mm proteasome $\alpha\beta$ but not with Mm proteasome $\alpha m\beta 1$ or mock (Fig. 3*B*). These facts strongly suggest that the catalytic center in the Mm proteasome β-subunit is important to accelerate the degradation of mutant SOD1 proteins.

M. mazei Proteasome Reduces Cellular Toxicities of Mutant Superoxide Dismutase-1—Next, we investigated the viability of HEK293 cells evoked by SOD1 (wild-type, $SOD1^{G93A}$, and $SOD1^{G85R}$) when co-expressed with Mm proteasome $\alpha\beta$, $\alpha m\beta 1$, or mock by the MTS-based cell proliferation assay (Fig. 4). We confirmed a linear response between cell number and optical density at 490 nm between 0.85 and 1.30 (data not shown). The viability of cells expressing wild-type SOD1 with Mm proteasome $\alpha\beta$ did not change as the transfected DNA doses of SOD1 and Mm proteasome $\alpha\beta$ increased (Fig. 4*A*). However, the viability of cells expressing mutant SOD1 was reduced as the transfected DNA dose of SOD1 increased (Fig. 4, *B* and *C*), and this reduction was prevented by the co-transfection with Mm proteasome $\alpha\beta$ but not with Mm proteasome $\alpha m\beta 1$. Toxicities of mutant SOD1 proteins are associated with the activation of caspase family proteins, especially caspase-3 (21). Using fluorescent substrates of activated caspase-3/7 as markers, we analyzed caspase-3/7 activities in the cells co-transfected with SOD1 proteins and with mock, Mm proteasome $\alpha\beta$, and $\alpha m\beta 1$. Mm proteasome $\alpha\beta$ suppressed the activation of caspase-3/7, resulting in reductions of cellular toxicities of SOD1 proteins (Fig. 4*D*). These results show that Mm proteasome $\alpha\beta$ has a protective effect against the decrease in cellular viability evoked by mutant SOD1.

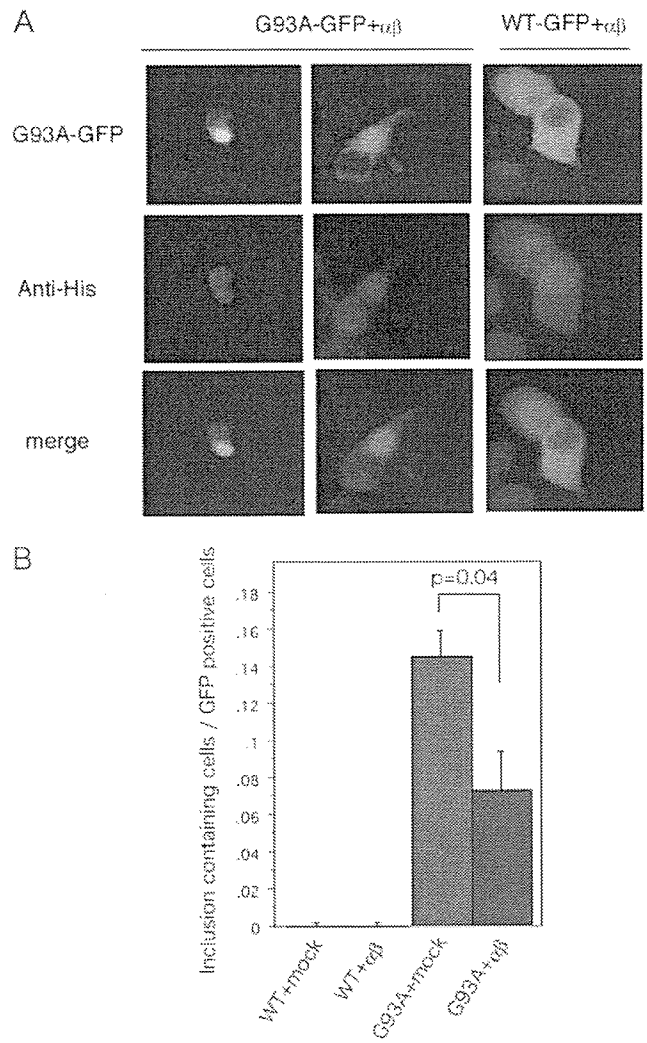

FIGURE 5. **Co-localization of mutant SOD1 and *M. mazei* proteasomes.** *A*, Neuro2a cells grown on glass coverslips were co-transfected with $SOD1^{WT}$-GFP or $SOD1^{G93A}$-GFP and Mm proteasome α- and His-tagged β-subunit. 48 h after transfection, cells were fixed, blocked, and incubated with anti-His antibody for 24 h. After washing, samples were incubated with Alexa-546-conjugated anti-mouse antibody. $SOD1^{G93A}$ and the Mm proteasome co-localized and formed aggregates together. *WT*, wild-type SOD1; *G93A*, $SOD1^{G93A}$. *B*, the percentages of aggregate-positive cells among the GFP-positive cells were determined. $SOD1^{G93A}$ aggregates were significantly reduced when co-expressed with Mm proteasome $\alpha\beta$. *Error bars*, S.D. ($n = 3$). Statistical analyses were carried out by Mann-Whitney's *U* test.

M. mazei Proteasome Co-localizes with Aggregates Formed by Mutant SOD1—In the assembly process of the archaeal proteasome, α-subunit assembly is required for β-subunit incorporation into the proteasome (20), and since the anti-His-stained β-subunit is restricted largely to that incorporated into the Mm proteasome (Fig. 1*E*), we used anti-His staining to localize the transfected proteasome in Neuro2a cells. GFP-tagged wild-type and G93A mutant SOD1 vectors were transfected along with Mm proteasome $\alpha\beta$ into Neuro2a cells, which were then fixed and immunostained with anti-His antibody. Fig. 5*A* shows that

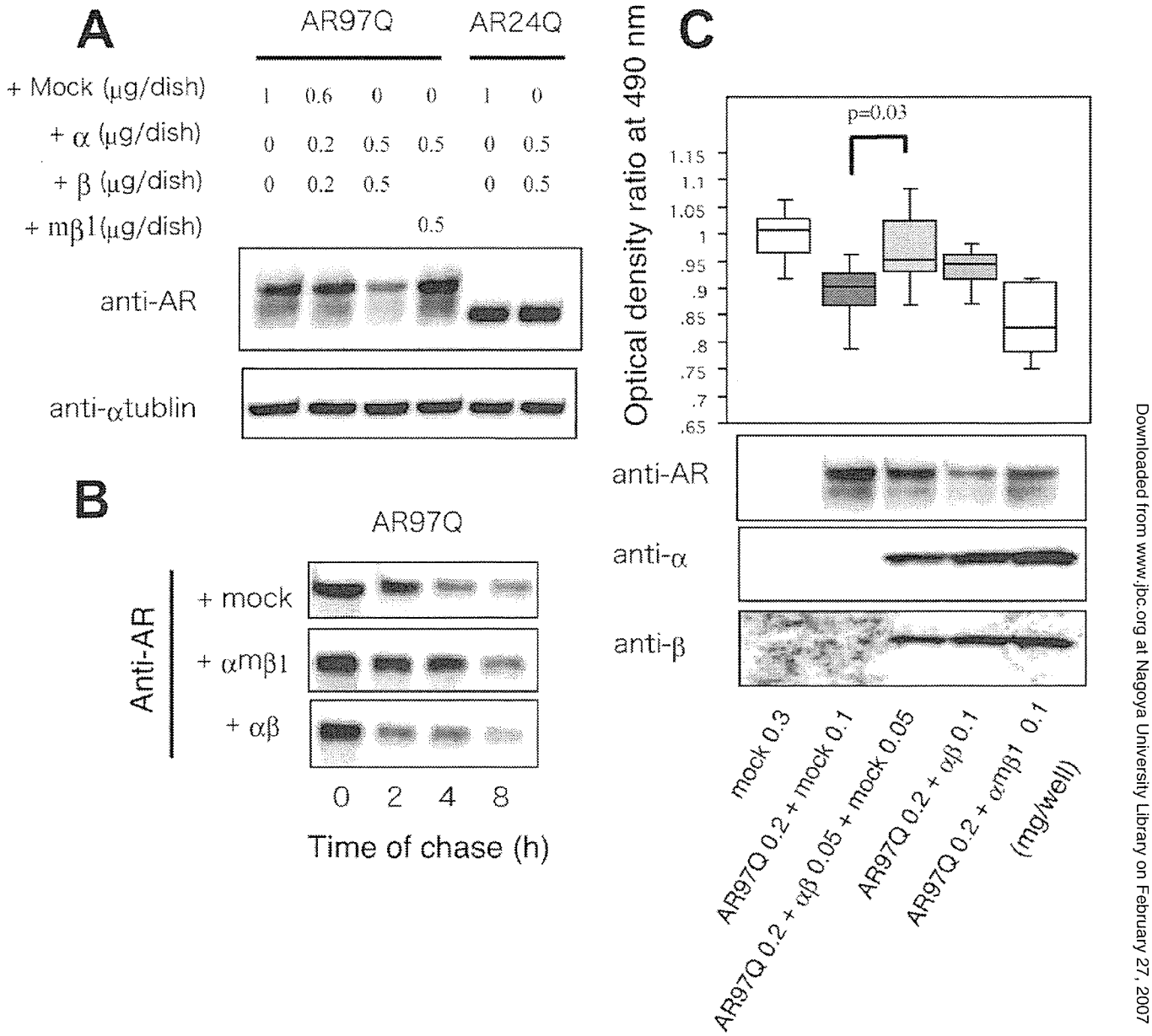

FIGURE 6. ***M. mazei* proteasome degrades mutant androgen receptor with expanded polyglutamine tract and reduces its cellular toxicity.** *A*, Neuro2a cells grown on 6-cm dishes and co-transfected with 1 μg of AR containing either normal (24Q) or expanded (97Q) polyglutamine tract vectors and increasing doses of Mm proteasome subunits were analyzed. The levels of AR^{97Q} proteins were reduced as Mm proteasome αβ increased. *B*, cycloheximide chase analysis (see "Experimental Procedures") showing that the half-lives of AR^{97Q} proteins were decreased in the presence of Mm 20 S proteasome αβ. Transfected DNA dose/6-cm dish was as follows: AR^{97Q} (1 μg), α-subunit (0.5 μg), β-subunit (0.5 μg). *C*, the rescue effect of Mm proteasome αβ expression on cell viability in AR^{97Q}-transfected HEK293 cells as shown in an MTS assay. The *box plots* show the median values (*center line* of *box*), the 25th (*lower line* of *box*), 75th (*upper line* of *box*), 10th (*lower T bar*), and 90th (*upper T bar*) percentiles in each group ($n = 3 \times 6$ wells). The *numbers* indicate transfected DNA dose in a well of a 96-well plate (αβ, 0.1 μg; α, 0.05 μg; β, 0.05 μg). The expression levels of AR, α-subunit, and β-subunit at analyzed points are shown.

GFP-positive $SOD1^{G93A}$ aggregates are also anti-His positive, whereas the cells expressing wild-type SOD1-GFP are diffusely stained with anti-His antibody. There were no GFP-negative inclusion bodies stained with anti-His antibody, indicating that Mm proteasome co-localizes with the inclusion bodies consisting of mutant SOD1 in the vicinity of the nucleus. The percentages of aggregate-positive cells among the GFP-positive cells were determined in Fig. 5*B*. $SOD1^{G93A}$ aggregates were significantly reduced when co-expressed with Mm proteasome αβ.

M. mazei Proteasome Degrades Specifically Mutant Androgen Receptor with Expanded Polyglutamine Tract and Reduces Its Cellular Toxicity—To demonstrate the ability of the Mm proteasome to degrade aggregation-prone proteins, we examined the AR with expanded polyglutamine tract (97-repeated glutamine; 97Q) protein, the causative protein of spinal and bulbar muscular atrophy. Similar to the results obtained with SOD1 proteins, Fig. 6*A* shows that in Neuro2a cells, the levels of mutant AR (97Q) were markedly reduced as the expression of

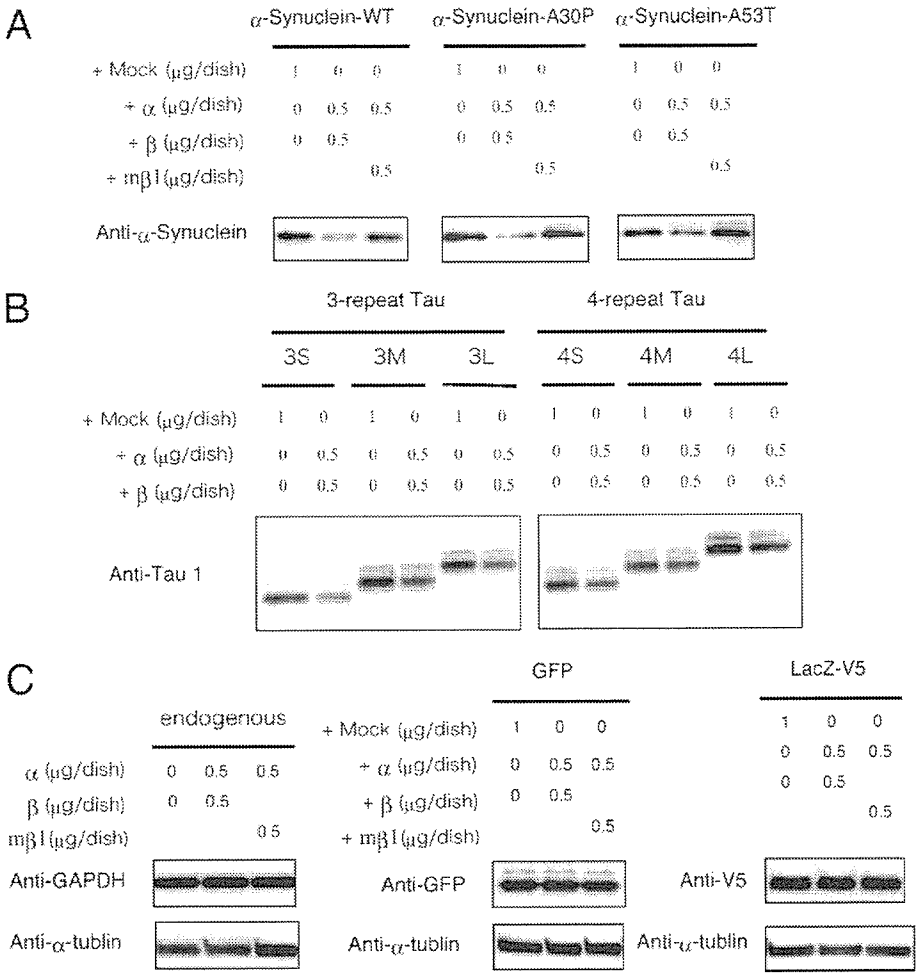

FIGURE 7. ***M. mazei*** **proteasome degrades aggregation-prone but not non-aggregation-prone proteins.** Neuro2a cells grown on 6-cm dishes and co-transfected with Mm proteasome subunits vectors or mock and 1 μg of α-synuclein vectors (wild type, A30P, and A53T) (*A*), Tau vectors (six isoforms: three (3L, 3M, and 3S) or four (4L, 4M, and 4S) tubulin binding domains in the C-terminal portion and two (3L and 4L), one (3M and 4M), or no (3S and 4S) inserts of 29 amino acids each in the N-terminal portion) (*B*), or empty GFP vector or LacZ-V5 vector (*C*). *A* and *B*, the expression levels of all of α-synuclein and tau proteins were reduced when co-transfected with the Mm proteasome αβ. *C*, the expression levels of endogenous glyceraldehyde-3-phosphate dehydrogenase (*GAPDH*), GFP, and LacZ-V5 proteins were not changed in the presence of the Mm proteasome αβ.

Mm proteasome αβ increased, but they were unaffected by the expression of the Mm proteasome αmβ1. On the other hand, wild-type AR (24-repeated glutamine; 24Q) levels were not affected by the expression of Mm proteasome αβ. Cycloheximide-chasing analysis demonstrated that the half-life of mutant AR (97Q) was reduced in the presence of the Mm proteasome but not in the presence of the mutant Mm proteasome (Fig. 6*B*). The viability of cells expressing mutant AR (97Q) was reduced compared with wild-type AR (24Q), and this reduction was attenuated by the co-transfection with Mm proteasome αβ (Fig. 6*C*). These results show that Mm proteasome αβ can accelerate the degradation of the aggregation-prone mutant AR with expanded polyglutamine tract and possibly protect the cells from its toxicities.

M. mazei Proteasome Degrades Other Aggregation-prone Proteins but Not Non-aggregation-prone Proteins—To determine whether the Mm proteasome degrades other aggregation-prone proteins as well, we examined its effects on α-synuclein (wild-type, A53T, and A30P) and six isoforms of wild-type tau protein in Neuro2a cells. The six tau isoforms contained either three (3L, 3M, and 3S) or four (4L, 4M, and 4S) microtubule binding domains in the C-terminal portion and two (3L, 4L), one (3M, 4M), or no (3S, 4S) inserts of 29 amino acids each in the N-terminal portion. Similar to the results obtained with the mutant SOD1 and AR with an expanded polyglutamine tract, the expression levels of all α-synuclein and tau proteins were reduced in the presence of Mm proteasome αβ (Fig. 7, *A* and *B*). Although the degradations of wild-type SOD1 and AR proteins were not accelerated by Mm proteasome, the expression levels of α-synuclein including wild-type and all of the six forms of wild-type tau were reduced.

We also examined whether Mm proteasomes degrade non-aggregation-prone proteins such as GFP or LacZ. Fig. 7*C* shows that the Mm proteasome does not affect the degradation of the exogenously expressed proteins, GFP and LacZ.

DISCUSSION

In this study, we showed that the archaeal Mm proteasome α- and β-subunits properly assembled to have proteolytic activity and accelerate the degradation of aggregation-prone, neurodegeneration-associated proteins in mammalian cells. Archaeal proteasomes contain 14 identical active sites that, although originally classified as chymotrypsin-like, were later shown to cleave after acidic and basic residues (22), and they consist of only one type of each of the α- and β-subunits (6). A comparison between archaeal and eukaryotic proteasomes *in vitro* showed that archaeal proteasomes are far more active in degrading poly(Q) peptides than are eukaryotic proteasomes (9). We utilized this potential power and manageability of archaeal proteasomes to degrade abnormal proteins that could not be effectively degraded by eukaryotic proteasomes. This is the first report showing that archaeal proteasomes can work to accelerate degradation of aggregation-prone proteins in mammalian cells.

Mm proteasomes promoted degradation of mutant SOD1, AR with an expanded polyglutamine tract, wild-type and mutant α-synuclein, and six isoforms of wild-type tau. The first two proteins, mutant SOD1 and AR with an expanded polyglutamine tract, exhibit toxicity in cell culture models. Mice over-expressing these mutant proteins display abnormal aggrega-

tions in their motor neurons and significant loss of motor functions, and they have been used as disease models (23, 24). Mm proteasomes accelerated the degradation of only the mutant forms of these two proteins and not that of the nonaggregating wild-type forms. Furthermore, chasing studies (Fig. 3, *A* and *B*) confirmed our belief that Mm proteasomes directly accelerate the degradation of mutant proteins.

However, both the wild-type and two mutants of α-synuclein as well as six isoforms of wild-type tau were also degraded by Mm proteasomes (Fig. 7). α-Synuclein and tau are pathogenically different proteins from SOD1 and AR, since they are known to accumulate as wild-type proteins in the affected lesions of PD and AD, respectively. Aggregation of the presynaptic protein, α-synuclein, has been implicated in synucleinopathies, such as sporadic and familial PD, diffuse Lewy body disease, and multiple-system atrophy (25). In sporadic PD patients, wild-type α-synuclein is accumulated, and increased expression of wild-type α-synuclein is also observed (26). Proteasomal dysfunction has been thought to impair α-synuclein degradation and thereby to facilitate its aggregation (27). Three- and four-repeat wild-type tau are among the proteins characteristically detected in neurofibrillary tangles formed by paired helical filaments in sporadic AD (28). Decreased proteasomal activity has been also reported in the AD brain (29). α-Synuclein and tau are both relatively easily misfolded, which leads to the formation of aggregates, even in their wild-type forms (30, 31), thus possibly explaining why the Mm proteasomes degraded wild-type α-synuclein and tau. Mm proteasomes might be able to recognize a wide range of aggregation-prone proteins, whereas they do not affect the degradation of exogenously expressed nonaggregating proteins, such as GFP and LacZ, or abundant endogenous proteins, such as α-tubulin and glyceraldehyde-3-phosphate dehydrogenase (Fig. 7).

The question raised here is what is the molecular mechanism of such selective, mutant species-dependant degradation. Archaeal 20 S proteasomes contain proteasome-activating nucleotidase, PAN, enabling substrates to enter the proteasomes easily and effectively (8). PAN has a chaperone-like activity to unfold aggregated proteins (32) and is thought to be an evolutionary precursor to the 19 S base in eukaryotic cells (8). Archaeal recognition tags (like ubiquitin tags in eukaryotic cells) have not been identified yet. However, archaeal 20 S proteasomes have been reported to rapidly degrade polyglutamine aggregates *in vitro*, without the help of PAN (9). Here we confirmed that this PAN-independent degradation by Mm 20 S proteasomes could occur in mammalian cells. Since the pore diameter of the closed gate in 20 S proteasomes is estimated to be much smaller than that of aggregated proteins (33), the question is, how do the unfolded substrate proteins enter the 20 S proteasomes? One hypothesis might be that the α-ring in Mm proteasomes has chaperone-like activity to recognize and unfold the aggregation-prone proteins or misfolded proteins. The gated channel in the α-ring of the archaeal 20 S proteasomes is thought to regulate substrate entry into the proteasomes and is assumed to be in either an open (34) or a closed state (2, 33) *in vitro*. In our experiments, the gate-free Mm 20 S proteasome Δαβ substantially reduced cell viability, but the Mm proteasome αβ, with the "gate," had little toxic effect on the cells and, furthermore, accelerated the degradation of mutant proteins. This would be hard to explain if the gate is always in the closed state. There is a possibility that when Mm proteasomes gather, actively or passively, near aggregation-prone proteins, the α-ring opens its gate and unfolds the aggregated proteins, enabling them to enter the proteasomes to be degraded.

Some kinds of molecular chaperones, such as Hsp90, -70, and -27, have been reported to assist in the selective degradation of mutant SOD1 and AR proteins in proteasome degradation pathways (35, 17). However, neither the protein levels of molecular chaperones (Hsp90, -70, -40, and -27) nor the ubiquitylation levels of mutant SOD1 and AR were changed in the presence of Mm proteasome αβ expression (data not shown), thus supporting the idea that endogenous ubiquitin-proteasome degradation pathways possibly did not play an important role in the accelerated degradation of mutant proteins. Further study is needed to elucidate the molecular mechanisms of selective recognition of misfolded aggregation-prone proteins by Mm proteasomes.

In this paper, we demonstrated that Mm proteasomes could effectively degrade neurodegenerative disease-related aggregation-prone proteins *in vivo*. Further studies are needed to determine whether archaeal proteasomes can be available to treat diseases in which toxic gain of proteins is causative.

Acknowledgments—We are grateful to Dr. Keiji Tanaka (Tokyo Metropolitan Institute for Medical Science) and Dr. Peter Zwickl (Max-Planck-Institut fur Biochemie, Abteilung Molekulare Strukturbiologie) for invaluable support for this study and for preparing the manuscript.

REFERENCES

1. Hershko, A., and Ciechanover, A. (1998) *Annu. Rev. Biochem.* **67,** 425–479
2. Puhler, G., Weinkauf, S., Bachmann, L., Muller, S., Engel, A., Hegerl, R., and Baumeister, W. (1992) *EMBO J.* **11,** 1607–1616
3. Zwickl, P., Kleinz, J., and Baumeister, W. (1994) *Nat. Struct. Biol.* **1,** 765–770
4. Seemüller, E., Lupas, A., Stock, D., Lowe, J., Huber, R., and Baumeister, W. (1995) *Science* **268,** 579–582
5. Grziwa, A., Baumeister, W., Dahlmann, B., and Kopp, F. (1991) *FEBS Lett.* **290,** 186–190
6. Baumeister, W., Walz, J., Zuhl, F., and Seemüller, E. (1998) *Cell* **92,** 367–380
7. Zwickl, P., Goldberg, A. L., and Baumeister, W. (2000) *Proteasomes: The World of Regulatory Proteolysis*, pp. 8–20, Landes Bioscience, Georgetown, TX
8. Zwickl, P., Ng, D., Woo, K. M., Klenk, H. P., and Goldberg, A. L. (1999) *J. Biol. Chem.* **274,** 26008–26014
9. Venkatraman, P., Wetzel, R., Tanaka, M., Nukina, N., and Goldberg, A. L. (2004) *Mol. Cell* **14,** 95–104
10. Ciechanover, A., Orian, A., and Schwartz, A. L. (2000) *J. Cell. Biochem.* **77,** 40–51
11. Kabashi, E., Agar, J. N., Taylor, D. M., Minotti, S., and Durham, H. D. (2004) *J. Neurochem.* **89,** 1325–1335
12. Bailey, C. K., Andriola, I. F., Kampinga, H. H., and Merry, D. E. (2002) *Hum. Mol. Genet.* **11,** 515–523
13. Chen, Q., Thorpe, J., and Keller, J. N. (2005) *J. Biol. Chem.* **26,** 30009–30017
14. Keck, S., Nitsch, R., Grune, T., and Ullrich, O. (2003) *J. Neurochem.* **85,** 115–122

15. Bence, N. F., Sampat, R. M., and Kopito, R. R. (2001) *Science* **292,** 1552–1555
16. Niwa, J., Ishigaki, S., Hishikawa, N., Yamamoto, M., Doyu, M., Murata, S., Tanaka, K., Taniguchi, N., and Sobue, G. (2002) *J. Biol. Chem.* **277,** 36793–36798
17. Waza, M., Adachi, H., Katsuno, M., Minamiyama, M., Sang, C., Tanaka, F., Inukai, A., Doyu, M., and Sobue, G. (2005) *Nat. Med.* **11,** 1088–1095
18. Ito, T., Niwa, J., Hishikawa, N., Ishigaki, S., Doyu, M., and Sobue, G. (2003) *J. Biol. Chem.* **278,** 29106–29114
19. Benaroudj, N., Zwick, P., Seemüller, E., Baumeister, W., and Goldberg, A. L. (2003) *Mol. Cell* **11,** 69–78
20. Seemüller, E., Lupas, A., and Baumeister, W. (1996) *Nature* **382,** 468–471
21. Sathasivam, S., Grierson, A. J., and Shaw, P. J. (2005) *Neuropathol. Appl. Neurobiol.* **31,** 467–485
22. Dahlmann, B., Kopp, F., Kuehn, L., Hegerl, R., Pfeifer, G., and Baumeister, W. (1991) *Biomed. Biochim. Acta* **50,** 465–469
23. Gurney, M. E., Pu, H., Chiu, A. Y., Dal Canto, M. C., Polchow, C. Y., Alexander, D. D., Caliendo, J., Hentati, A., Kwon, Y. W., Deng, H. X., Chen, W., Zhai, F., Sufit, R. L., and Siddique, T. (1994) *Science* **264,** 1772–1775
24. Adachi, H., Kume, A., Li, M., Nakagomi, Y., Niwa, H., Do, J., Sang, C., Kobayashi, Y., Doyu, M., and Sobue, G. (2001) *Hum. Mol. Genet.* **10,** 1039–1048
25. Trojanowski, J. Q., and Lee, V. M. (2003) *Ann. N. Y. Acad. Sci.* **991,** 107–110
26. Miller, D. W., Hague, S. M., Clarimon, J., Baptista, M., Gwinn-Hardy, K., Cookson, M. R., and Singleton, A. B. (2004) *Neurology* **62,** 1835–1838
27. Liu, C. W., Corboy, M. J., DeMartino, G. N., and Thomas, P. J. (2003) *Science* **299,** 408–411
28. Selkoe, D. J. (1991) *Neuron* **6,** 487–498
29. Keller, J. N., Hanni, K. B., and Markesbery, W. R. (2000) *J. Neurochem.* **75,** 436–439
30. Hashimoto, M., Hsu, L. J., Sisk, A., Xia, Y., Takeda, A., Sundsmo, M., and Masliah, E. (1998) *Brain Res.* **799,** 301–306
31. Khlistunova, I., Biernat, J., Wang, Y., Pickhardt, M., von Bergen, M., Gazova, Z., Mandelkow, E., and Mandelkow, E. M. (2006) *J. Biol. Chem.* **281,** 1205–1214
32. Benaroudj, N., and Goldberg, A. L. (2000) *Nat. Cell Biol.* **2,** 833–839
33. Groll, M., Bajorek, M., Kohler, A., Moroder, L., Rubin, D. M., Huber, R., Glickman, M. H., and Finley, D. (2000) *Nat. Struct. Biol.* **7,** 1062–1067
34. Lowe, J., Stock, D., Jap, B., Zwickl, P., Baumeister, W., and Huber, R. (1995) *Science* **268,** 533–539
35. Patel, Y. J., Payne Smith, M. D., de Belleroche, J., and Latchman, D. S. (2005) *Brain Res. Mol. Brain Res.* **134,** 256–274

Journal of Neuroscience Research 83:119–133 (2006)

Disease Progression of Human SOD1 (G93A) Transgenic ALS Model Rats

Arifumi Matsumoto,[1,3,6] Yohei Okada,[1,4,6] Masanori Nakamichi,[5] Masaya Nakamura,[2] Yoshiaki Toyama,[2] Gen Sobue,[4] Makiko Nagai,[3] Masashi Aoki,[3] Yasuto Itoyama,[3] and Hideyuki Okano[1,6]*

[1]Department of Physiology, Keio University School of Medicine, Tokyo, Japan
[2]Department of Orthopaedic Surgery, Keio University School of Medicine, Tokyo, Japan
[3]Department of Neurology, Tohoku University Graduate School of Medicine, Sendai, Japan
[4]Department of Neurology, Nagoya University Graduate School of Medicine, Nagoya, Japan
[5]Takeda Chemical Industries, Ltd., Osaka, Japan
[6]Core Research for Evolutional Science and Technology (CREST), Japan Science and Technology Agency (JST), Saitama, Japan

The recent development of a rat model of amyotrophic lateral sclerosis (ALS) in which the rats harbor a mutated human SOD1 (G93A) gene has greatly expanded the range of potential experiments, because the rats' large size permits biochemical analyses and therapeutic trials, such as the intrathecal injection of new drugs and stem cell transplantation. The precise nature of this disease model remains unclear. We described three disease phenotypes: the forelimb-, hindlimb-, and general-types. We also established a simple, non-invasive, and objective evaluation system using the body weight, inclined plane test, cage activity, automated motion analysis system (SCANET), and righting reflex. Moreover, we created a novel scale, the Motor score, which can be used with any phenotype and does not require special apparatuses. With these methods, we uniformly and quantitatively assessed the onset, progression, and disease duration, and clearly presented the variable clinical course of this model; disease progression after the onset was more aggressive in the forelimb-type than in the hindlimb-type. More importantly, the disease stages defined by our evaluation system correlated well with the loss of spinal motor neurons. In particular, the onset of muscle weakness coincided with the loss of approximately 50% of spinal motor neurons. This study should provide a valuable tool for future experiments to test potential ALS therapies.

Key words: amyotrophic lateral sclerosis; evaluation system; behavioral analyses; phenotype; variability

Amyotrophic lateral sclerosis (ALS) is a fatal neurodegenerative disorder that mainly affects the upper and lower motor neurons (de Belleroche et al., 1995). It is characterized by progressive muscle weakness, amyotrophy, and death from respiratory paralysis, usually within 3–5 years of onset (Brown 1995). Although most cases of ALS are sporadic (SALS), approximately 10% are familial (FALS) (Mulder et al., 1986). Moreover, 20–25% of FALS cases are due to mutations in the gene encoding copper-zinc superoxide dismutase (SOD1) (Deng et al., 1993; Rosen et al., 1993). More than 100 different mutations in the SOD1 gene have been identified in FALS so far.

Until recently, animal models of FALS have been various transgenic mice that express a mutant human SOD1 (hSOD1) gene. Of these, a transgenic mouse carrying the G93A (Gly-93 → Ala) mutant hSOD1 gene was the first described (Gurney et al., 1994) and is used all over the world because this model closely recapitulates the clinical and histopathological features of the human disease. To evaluate the therapeutic effects of potential ALS treatments in this animal, many motor-related behavioral tasks are used (Chiu et al., 1995; Barneoud et al., 1997; Garbuzova-Davis et al., 2002; Sun et al., 2002; Wang et al., 2002; Inoue et al., 2003; Kaspar et al., 2003; Weydt et al., 2003; Azzouz et al., 2004). However, transgenic mice have innate limitations for some types of experiments because of their small size.

Recently, transgenic rat models of ALS, which harbor the hSOD1 gene containing the H46R (His-46 → Arg) or G93A mutation were generated (Nagai et al., 2001). The larger size of these rat models makes certain experiments easier, such as biochemical analyses that require large amounts of sample, intrathecal administration

Contract grant sponsor: Core Research for Evolutional Science and Technology (CREST), Japan Science and Technology Agency (JST); Contract grant sponsor: Japanese Ministry of Health, Labour and Welfare; Contract grant sponsor: Japanese Ministry of Education, Culture, Sports, Science and Technology.

*Correspondence to: Hideyuki Okano, Department of Physiology, School of Medicine, Keio University, 35 Shinanomachi, Shinjuku-ku, Tokyo, 160-8582, Japan. E-mail: hidokano@sc.itc.keio.ac.jp

Received 22 August 2005; Revised 29 September 2005; Accepted 30 September 2005

Published online 7 December 2005 in Wiley InterScience (www.interscience.wiley.com). DOI: 10.1002/jnr.20708

of drugs, and, especially, therapeutic trials, including the transplantation of neural stem cells into the spinal cord. The hSOD1 (G93A) transgenic rats typically present weakness in one hindlimb first. Later, weakness progresses to the other hindlimb and to the forelimbs. Finally, the rats usually become unable to eat or drink, and eventually die. Only subjective and ambiguous analyses were made with regard to the clinical progression of this ALS animal model and objective criteria for evaluating the efficacy of these new treatments have not been determined. For these reasons, we assessed the disease progression quantitatively using five different measures (body weight, inclined plane test, cage activity, SCANET, and righting reflex) and established an easy, noninvasive, and objective evaluation system that is sensitive to small but important abnormalities in the hSOD1 (G93A) transgenic rats. In addition, we created a novel scale, the Motor score, to assess disease progression in the transgenic rats without using special apparatuses. We also examined the validity of these measures as assessment tools for the pathology by investigating the number of spinal motor neurons remaining at the disease stages defined by each measure.

MATERIALS AND METHODS

Transgenic Rats

All animal experiments were conducted according to the Guidelines for the Care and Use of Laboratory Animals of Keio University School of Medicine. We used hSOD1 (G93A) transgenic male rats (Nagai et al., 2001) from our colony and their age- and gender-matched wild-type littermates as controls. Rats were housed in a specific pathogen-free animal facility at a room temperature of 23 ± 1°C under a 12-hr light-dark cycle (light on at 08:00). Food (solid feed CE-2, 30kGy; CLEA Japan, Inc.) and water were available ad lib. Transgenic rats were bred and maintained as hemizygotes by mating transgenic males with wild-type females. Transgenic progeny were identified by detecting the exogenous hSOD1 transgene, by amplification of pup tail DNA extracted at 20 days of age by polymerase chain reaction (PCR). The primers and cycling conditions were described previously (Nagai et al., 2001).

Exploration of Assessment Tools to Measure Disease Progression in the hSOD1 (G93A) Transgenic Rats

We evaluated the usefulness of four different measures to assess disease progression in the transgenic rats. All tests were carried out between 12:00–16:00 and in a double-blind fashion.

Body weight. Animals ($n = 9$ for each genotype) were weighed weekly after 30 days of age with an electronic scale. To avoid overlooking the beginning of weight loss, the animals were weighed every second or third day after 90 days of age, the age at which motor neurons are reported to be lost in the lumbar spinal cord (Nagai et al., 2001).

Inclined plane. This test was initially established mainly to assess the total strength of the forelimbs and hindlimbs in a model of spinal cord injury (Rivlin and Tator, 1977). Briefly, rats were placed laterally against the long axis of the inclined plane, and the maximum angle at which they could maintain their position on the plane for 5 sec was measured. To assess the strength of both sides of limbs equally, animals were placed on the inclined plane with the right side of the body to the downhill side of the incline, and then with the left side of the body facing downhill. For each rat, the test was carried out three times for each side, and the mean value of the angles obtained for the right side was compared to that obtained for the left. The lower mean value was recorded as the angle for that rat. Animals ($n = 9$ for each genotype) were tested weekly after 70 days of age and every second to third day after 100 days of age.

Cage activity. Animals ($n = 8$ for each genotype) were housed individually and monitored every day for all 24 hr (except for the days the cages were changed) after they were 70 days old. Spontaneous locomotor activity in the home cage (345 × 403 × 177 mm) was recorded by an activity-monitoring system (NS-AS01; Neuroscience, Inc., Tokyo, Japan) as described previously (Ohki-Hamazaki et al., 1999). The sensor detects the movement of animals using the released infrared radiation associated with their body temperature. The data were analyzed by the DAS-008 software (Neuroscience, Inc., Tokyo, Japan). To eliminate data variability owing to differences in the baseline movement of each rat, the baseline value was calculated as the mean of movement from 70–90 days of age, during which all rats were considered to move normally. We analyzed the data at each time point as the percentage of the baseline value in defining disease onset with this test.

SCANET. For short-term activity, 10 min of spontaneous activity was measured with the automated motion analysis system SCANET MV-10 (Toyo Sangyo Co., Ltd., Toyama, Japan) (Mikami et al., 2002). Animals ($n = 4$ for each genotype) were tested weekly after 30 days of age and every second or third day after 100 days of age. Each rat was individually placed in the SCANET cage for 10 min. Three parameters were measured: small horizontal movements of 12 mm or more (Move 1; M1), large horizontal movements of 60 mm or more (Move 2; M2), and the frequency of vertical movements caused by rearing (RG). To distinguish RG movements from incomplete standing actions, the upper sensor frame was adjusted to 13 cm above the lower sensor frame.

Righting reflex. All affected animals were tested for the ability to right themselves within 30 sec of being turned on either side (righting reflex) (Gale et al., 1985). Failure was seen when animals reached the end-stage of disease (Howland et al., 2002), and was regarded as a generalized loss of motor activity. We used this time point, which we call "end-stage," as "death" rather than the actual death of the animal, to exclude the influence of poor food intake and respiratory muscle paralysis on the survival period. All end-stage animals were sacrificed after being deeply anesthetized.

All statistical analyses were carried out with the two-tailed unpaired Student's t-test. A P-value of <0.05 was considered statistically significant.

Motor Score

To establish our own scoring system for motor function, which could be uniformly applicable to any disease phenotype of this rat model, we examined the common clinical findings

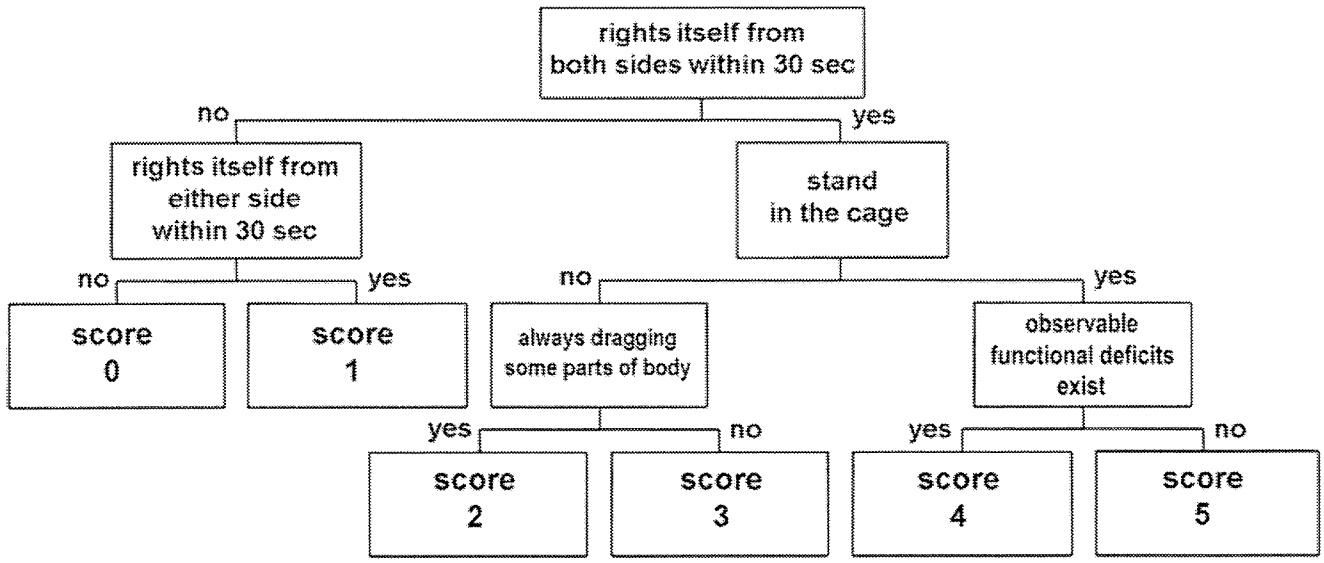

Fig. 1. Chart of Motor score assessment. The degree of motor dysfunction can be assessed by the Motor score as shown in this chart. This scoring system is meant to be used after disease onset, which can be prospectively diagnosed by the inclined plane test (muscle weakness onset). A score of 4 means the same condition as seen for subjective onset (SO). Rats with a score of 5 seem almost as normal as wild-type rats. The detailed testing procedure for the Motor score is described in the text.

of the transgenic rats in detail and assessed their motor functions ($n = 20$). We focused on the following tests: the righting reflex, the ability to stand in the cage, the extent of dragging their bodies when moving, and the existence of observable functional deficits. We evaluated these items sequentially along with the disease progression and classified the rats into six groups by giving them scores between 0 and 5. The scoring chart (Motor score) is shown in Figure 1.

When disease onset in the rats was diagnosed by their scoring $<70^{\circ}$ on the inclined plane test (muscle weakness onset), the affected rats were tested for righting reflex. If they were unable to right themselves from either side, they were given a score of 0. If they could right themselves from only one side but not the other, they were given a score of 1.

Rats that could right themselves from both sides were examined for the ability to stand in the cage as follows: Rats were observed in the home cage for 1 min to see if they would stand spontaneously (Step 1). When they moved little in the home cage or showed no tendency to stand during Step 1, they were stimulated by being transferred to another cage (Step 2), and then by being returned to their home cage again (Step 3); the transfers were done to activate exploration motivation. During Step 3, the rats were further stimulated by lightly knocking the cage to intensify the motivation to explore. Each step was carried out for 1 min and the test was stopped when the rat stood once. Rats were judged as "unable to stand" if they did not stand, even after all three steps.

Rats that did not stand were subjected to the next test in the open field, where the extent to which they dragged their bodies when moving was assessed. Those who always dragged and could not lift some parts of their bodies except for scrotums and tails at any time were given a score of 2. If they could lift their dragging parts off the ground for even a moment, they were given a score of 3. The phenotype of dragging the forelimbs was different from that of dragging the hindlimbs. As disease progressed, "forelimb-type" rats first began to touch the tips of their noses on the ground, and then began to drag their head and upper trunk as they moved backward with their hindlimbs. "Hindlimb-type" rats dragged their lower trunk and moved forward with their forelimbs.

Finally, rats that had no abnormality in the above-mentioned assessments were examined in detail to see whether they had any observable functional deficits such as paralysis of the limbs or symptoms of general muscle weakness (e.g., walking with a limp, sluggish movement) in the open field. This condition could be judged subjectively and was defined as subjective onset. Rats with any of these symptoms were given a score of 4; otherwise they were given a score of 5.

Because the scores were based on subjective judgment, they might vary depending on the examiner. To examine inter-rater variability, three transgenic rats of different clinical types were examined according to the method described above, recorded on video tape, and subsequently scored by five observers from different backgrounds (Table I). The scores classified by the five observers were statistically analyzed for inter-rater agreement using Cohen's κ statistics (Table II). Kappa values can range from 0 (no agreement) to 1.00 (perfect agreement), and can be interpreted as poor (<0.00), slight (0.00–0.20), fair (0.21–0.40), moderate (0.41–0.60), substantial (0.61–0.80), and almost perfect (0.81–1.00) (Landis and Koch, 1977). The scores for the three transgenic rats were, on the whole, quite consistent among the five observers, suggesting that the Motor score can be used as an objective method for assessing disease progression.

TABLE I. Motor Score of Transgenic Rats Assessed by Five Different Observers

		Days after onset (days)								
Transgenic rat	Observer	0	1	2	3	4	5	6	7	8
#1407 Eventual hindlimb type										
	A	5	4	4		2	2	1	0	
	B	4	4	4		2	2	1	0	
	C	4	4	4		2	2	1	0	
	D	4	4	4		2	2	1	0	
	E	4	4	4		2	2	1	0	
	Mean	4.2	4	4		2	2	1	0	
#1470 Pure hindlimb type										
	A	5		4	4	2	2	2	2	0
	B	5		4	3	3	2	2	2	0
	C	5		4	3	2	2	2	2	0
	D	4		4	4	2	2	2	2	0
	E	4		4	3	2	2	2	2	0
	Mean	4.6		4	3.4	2.2	2	2	2	0
#1449 Pure forelimb type										
	A	4	3	3	3		2	1	1	0
	B	4	3	3	3		2	1	1	0
	C	3	3	3	3		2	1	1	0
	D	3	3	3	3		2	1	1	0
	E	4	3	2	2		2	1	1	0
	Mean	3.6	3	2.8	2.8		2	1	1	0

TABLE II. The kappa Statistics for Inter-Rater Agreement of Motor Score

	Transgenic rat (clinical type)		
Observers	#1407 Eventual hindlimb	#1470 Pure hindlimb	#1449 Pure forelimb
A vs. B	0.82	0.69	1.00
A vs. C	0.82	0.82	0.83
A vs. D	0.82	0.81	0.83
A vs. E	0.82	0.70	0.69
B vs. C	1.00	0.83	0.83
B vs. D	1.00	0.53	0.83
B vs. E	1.00	0.66	0.69
C vs. D	1.00	0.64	1.00
C vs. E	1.00	0.82	0.54
D vs. E	1.00	0.81	0.54

TABLE III. Clinical Types of hSOD1 (G93A) Transgenic Rats

Clinical type	Subtype	*n*	%
Forelimb	Pure	4	8.2
	Eventual	5	10.2
Hindlimb	Pure	19	38.7
	Eventual	17	34.7
General		4	8.2
Total		49	100

Real-Time RT-PCR and Western Blot Analysis

Tissue specimens were dissected from the cerebral cortices, cerebella, medullae, and spinal cords (cervical, thoracic, and lumbar spinal cords) of the deeply anesthetized rats, and divided into two portions for total RNA and total protein preparation. Total RNA was isolated and first strand cDNA was synthesized as described previously (Okada et al., 2004). The real time RT-PCR analysis was carried out using Mx3000P (Stratagene, La Jolla, CA) with SYBR Premix Ex Taq (Takara Bio, Inc., Otsu, Japan). The primers used for the analysis were human *SOD1* (5′-TTGGGCAATGTGACTGCTGAC-3′, 5′-AGCTAGCAGGATAACAGATGA-3′), rat *SOD1* (5′-ACTTCGAGCAGAAGGCAAGC-3′, 5′-ACATTGGCCACACCGTCCTTTC-3′), and *β-actin* (5′-CGTGGGCCGCCCTAGGCACCA-3′, 5′-TTGGCCTTAGGGTTCAGAGGGG-3′). The results are presented as ratios of mRNA expression normalized to an inner control gene, *β-actin*. Total protein was prepared in lysis buffer containing 10 mM Tris-HCl (pH 7.6), 50 mM NaCl, 30 mM sodium pyrophosphate, 50 mM sodium fluoride, 20 mM glycerophosphate, 1% Triton X-100, and a protease inhibitor mixture (Complete; Roche Applied Science, Mannheim, Germany). Western blot analysis was carried out by a method established previously. In brief, a 5 μg protein sample of an extract was run on 12% SDS-PAGE, transferred to nitrocellulose, and probed with anti-human SOD1 (1:1,000, mouse IgG, Novocastra Laboratories, Ltd., Benton Lane, UK), and anti-α-tubulin (1:2,000, mouse IgG, Sigma-Aldrich, Inc., Saint Louis, MO). Signals were detected with HRP-conjugated secondary antibodies (Jackson ImmunoResearch Laboratories, Inc., West Grove, PA) using an ECL kit (Amersham Bioscience UK limited, Little Chalfont, UK). Quantitative analysis was carried out with a Scion Image (Scion Corporation, Frederick, MD). The amounts of proteins loaded in each slot were normalized to those of α-tubulin.

Immunohistochemical Analysis

Rats were deeply anesthetized (ketamine 75 mg/kg, xylazine 10 mg/kg, i.p.) and transcardially perfused with 4% paraformaldehyde/PBS (0.1 M PBS, pH 7.4) for histological examination. Spinal cord tissues were dissected out and post-fixed overnight in the same solution. Each spinal cord was dissected into segments that included the C6, T5, and L3 levels, immersed in 15% sucrose/PBS followed by 30% sucrose/PBS at 4°C, and embedded in Tissue-Tek O.C.T. Compound (Sakura Finetechnical Co., Ltd., Tokyo, Japan). Embedded tissue was immediately frozen with liquid nitrogen and stored at −80°C. Serial transverse sections of each spinal segment were cut on a cryostat at a thickness of 14 μm. The sections were pre-treated with acetone for 5 min, rinsed with PBS three times and permeabilized with TBST (Tris-buffered saline with 1% Tween 20) for 15 min at room temperature. After being blocked in the TNB buffer (Perkin-Elmer Life Sciences, Inc., Boston, MA) for 1 hr at room temperature, the sections were incubated at 4°C overnight with an anti-choline acetyltransferase (ChAT) polyclonal antibody (AB144P, Goat IgG, 1:50; Chemicon International, Inc., Temecula, CA). After being washed with PBS three times, the sections were incubated for 2 hr at room temperature with a biotinylated secondary antibody (Jackson ImmunoResearch Laboratories, Inc.). Finally, the labeling was developed using the avidin-biotin-peroxidase complex procedure (Vectastain ABC kits; Vector Laboratories, Inc., Burlingame, CA) with 3,3-diaminobenzidine (DAB; Wako Pure Chemical Industries, Ltd., Osaka, Japan) as the chro-